University of Milano - Bicocca
Department of Materials Science

Thermoplastic Elastomers from Chlorinated Polyethylene/Nylon Terpolyamide Blends

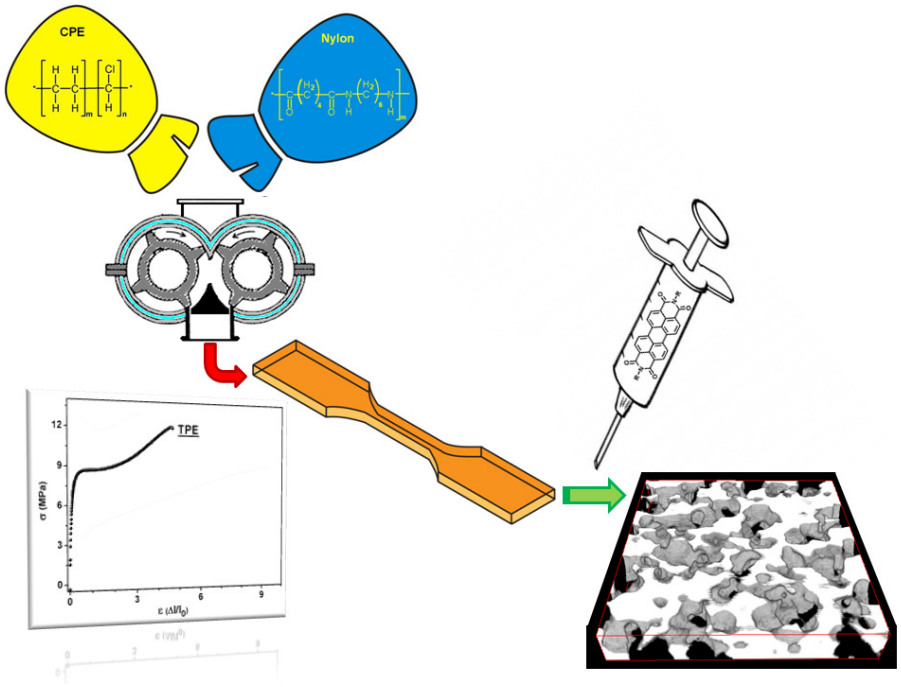

Tommaso Crisenza

Ph. D. School in Materials Science – XXIV cycle

Thesis presented for the degree of Doctor Europaeus

Supervisor: Dr. Roberto Simonutti

Dean of the Doctorate: Prof. Gian Paolo Brivio

January 2012

Non Discitur
Nisi Gradatim.

Contents

Abstract and Motivation

Blends of chlorinated polyethylene (CPE) and Nylon terpolyamide (PA) were prepared with different ratios. It is generally known that CPE has intrinsic properties of heat, oil and oxidation resistance, so the obtained materials are well suitable in the hose, pipe and seal industry. CPE was strengthened by a 6,6-6,12 co-polyamide with the glass transition temperature slightly above room temperature and a particularly low melting temperature, that allowed to obtain the blends by typical industrial processes of mixing, milling and injection molding. Mechanical and rheological properties were investigated both with tensile tests and dynamic mechanical analysis: the results showed that CPE and PA form phase separated systems with excellent compatibility as the strength and modulus were improved. The thermal and mechanical behavior of the blends is that typical of thermoplastic elastomers. The comparison of the FTIR spectra of the blends in respect of linear combination of those of the component polymers allowed the detection of differences attributed to the existence of interactions at the interface responsible of the enhanced mechanical properties. These results were corroborated by time-domain proton NMR experiments, with an improved method for the measurement of the hard/soft ratio in phase separated systems. With the aim to resolve the morphology of the blends, samples were studied with laser scanning confocal fluorescent microscopy (LSCFM). CPE rubber was homogeneously labeled with a fluorescent dye by solution treatment and then blended with PA in order to increase the contrast between phases in fluorescent microscopy. Scanning Electron Microscopy and Atomic Force Microscopy techniques were used to confirm the data collected with LSCFM. A continuous and interpenetrating structure of the two phases is finally revealed for the blend with the best mechanical properties.

Blends with co-continuous structures may combine the properties of both components in a favorable way. For example, a co-continuous structure leads to the maximum contribution of the mechanical modulus from each component simultaneously. Synergistic effects have also been shown in mechanical properties. Constituting a stable co-continuous morphology just mixing two polymers it is not that easy, and even more difficult is to detect such microstructure within the bulk of the material. For these two reasons, co-continuous polymer blends are an interesting and challenging research topic. In addition, these co-continuous structures offer promising opportunities for improving properties and creating tailor-made materials.

For these reason, and also as very few examples of Thermoplastic elastomers based on Chlorinated polyethylene and Nylon are present in the literature, the project for this thesis came to life. This work is aimed at the achievement of a material with thermoplastic elastomeric mechanical and processing properties, for which the structure properties relationships would be completely understood and explained as due to synergistic interfacial interaction between phases and co-continuous morphology within them.

1 Chapter One: Introduction

The outstanding advantage of thermoplastic elastomers can be summarized in a single sentence: *they allow rubber like materials to be produced using the rapid processing techniques developed by the thermoplastic industry*.[1]

This remarkable characteristic and their huge commercial development in the last decades, make thermoplastic elastomers an intensively investigated class of materials, both in industry and in academia.

1.1 Introduction to Thermoplastic Elastomers

The emergence of thermoplastic elastomers (TPEs) provided a new horizon to the field of polymer technology. Their development and growth have reached a high level of commercial significance, and they have become an important segment of polymer science and technology in the last four decades.[2]

In simplest way, thermoplastic elastomers can be defined as a class of polymers, which combine the service properties of elastomers with the processing properties of thermoplastic. TPEs are, in general, phase separated systems by definition; one phase is soft in nature and is above its glass transition temperature (T_g) at the service temperature of the final material, the other phase is crystalline and/or hard with an higher T_g, anyway below its T_g at the service temperature. This second phase acts as physical cross-link for the soft portion. These two phases must be thermodynamically immiscible to prevent the interpenetration.[3]

The physical cross-links given by the hard phase are thermo reversible, and this allows TPEs to soften and flow under shear force at elevated temperature as in case of true thermoplastic. Once cooled, the elastomeric portion provide TPEs the final rubber-like mechanical properties.

As shown in Table 1.1,[4] TPEs bridge the gap between conventional rubbers and thermoplastic.

Table 1.1: Comparison of thermoplastic elastomers with conventional plastics and rubbers.

	Thermosetting	Thermoplastic
Rigid	Epoxies Phenol-Formaldehyde Urea-Formaldehyde Bakelite	Polystyrene Polypropylene Polyvinyl chloride High Density Polyethylene
Flexible	Highly filled and/or highly vulcanized rubber	Low density polyethylene Poly (Ethylene-Vinyl Acetate) Plasticized Polyvinyl Chloride
Rubbery	Vulcanized rubbers (Natural Rubber, Styrene Butadiene Rubber, Nitrile Rubber, etc…)	**Thermoplastic Elastomers**

Mixing and blending a rubber with a plastic represents a basic way for obtaining thermoplastic elastomers.[5]

The blending of two or more polymers has gained considerable importance in recent years because the blends may give rise to certain properties that cannot be attained by other means or from individual components.[6] Thus thermoplastic elastomers can be prepared by mixing a thermoplastic and an elastomer under high shearing action.

Besides having low cost, these blends have certain advantages over other types of TPEs: in this class, the desired properties can be achieved by suitable selection of both rubber and plastic and their ratio in the blend.[7]

1.2 Historical remarks

The history of thermoplastic elastomers is inevitably part of the development of the whole history of polymer chemistry .[8] Moreover, knowing the recent developments of this class of materials should be helpful to better understand its nature and the way thermoplastic elastomers work.

Although natural polymers (e.g., cotton, wool, natural rubber) have been known for centuries, there was no understanding of the nature of these materials. Probably the first significant attempt to improve on nature was the cross-linking (or vulcanization) of the natural rubber, developed by Charles Goodyear in 1839. A few years before this, John Hancock reduced the molecular weight of rubber by milling. These two discoveries became the foundation of the rubber industry: despite the lack of fundamental understanding of the principles involved in these innovations, from this point many important discoveries continued to be made in the centuries, so the history of thermoplastic elastomers might start from here.

The very first seminal works made on thermoplastic elastomers were the development of plasticized polyvinyl chloride (PVC) in 1933 and the synthesis of polyurethanes starting from 1937.[9] The PVC is an halogenated polyolefin, a rigid thermoplastic, with a significant amount of syndiotactic structure that can crystallize but also atactic structure which remains amorphous. At room temperature the syndiotactic structure is crystalline and the atactic amorphous structure is above its glass transition temperature. Thus, both phases are hard and rigid at room temperature. However, by adding a plasticizer (e.g., dioctyl phthalate (DOP)) that swell the atactic polymer reducing its T_g to well below room temperature, one can obtain a flexible product. The result is what is defined, as explained before, as the structure of most thermoplastic elastomers: a combination of a rigid phase that becomes fluid at processing temperatures with a softer, flexible phase. Plasticized PVC is not usually considered an elastomer, but is the first material that even came close to being a thermoplastic elastomer; in

particular, its elastic properties were improved within the years by blending with another elastomer, the nitrile rubber (NBR): PVC/NBR/DOP blends are now an important part of the thermoplastic elastomers industry. About 1937, the urethane reaction between an isocyanate and an alcohol was developed. By using diisocyanates and glycols the result was a long chain structure, similar in principle to Nylon. By using two glycols (one short chain, the other long), blocks of two polyurethanes are produced; the first is crystalline, the second amorphous: again, they form the basic two phase system characteristic of most thermoplastic elastomers.

Besides these two developments, that can be consider as the roots of the TPE class of materials, other two scientific discoveries, both from the early 1960s, have to be cited as responsible for the origin of the TPEs: the anionic polymerization and the Ziegler-Natta catalysis. In the anionic polymerization, solution polymerization is initiated by a metallic anion: the system is "living", thus, in the absence of terminal agents, the polymeric product can polymerize further monomers. If a second monomer is added to the reaction mixture the result is a block copolymer. Shell Chemical was the first to present, in 1961, styrenic block copolymers. These were extremely important, as their simple and unequivocal structure gave a clear picture of how other thermoplastic elastomers (or at least, those based on block copolymers) gained their properties. Few years later, the Symposium on TPE theory at the California Institute of Technologies on 1967, combined with the outstanding publications by Legge et. Al.[10,4] laid the foundations, from the scientific standpoint, for the deep understanding and thus the study and the aware development of this class of materials.

The basic requirements for a thermoplastic elastomer, a hard phase and an elastomeric phase non miscible, were now established. As well as hard polymer/elastomer block copolymers, there are several other ways of achieving this requirement. An obvious one is simple mixing. Two new polymers (both

produced by Ziegler-Natta catalysts) were introduced. The first was a rubber, a copolymer of ethylene and propylene (EPM) and the second was a thermoplastic, isotactic polypropylene (iPP). When EPM was added, in conspicuous portion, to iPP, often extended with oil, the result was a thermoplastic elastomer. This material was further improved, around 1975, by the introduction as elastomeric phase of ethylene-propylene-diene rubber (EPDM), cross-linked during the mixing process in a system called "dynamic vulcanization". The resulting thermoplastic elastomers can be quite soft and their properties are often better than those of simple mixtures.

Concerning the hard polymer/elastomer melt mixed blends (both the simple mixtures and the one obtained by dynamic vulcanization) starting from 1978, Coran et. Al. from Monsanto company, carried a deep and complete study on this family of thermoplastic elastomers.[11,12,13,14,15,16,17,18,19] Respectively in 1981 and 1985, were introduced to the market from Monsanto new materials developed from rubber/plastic blends as EPDM/iPP dynamically vulcanized blends (Santoprene), and NBR/iPP dynamically vulcanized blends (Geolast).

Other system investigated include graft copolymers (an elastomer chain on which are covalently grafted several hard segments) and elastomeric ionomers (an elastomer chain containing acidic groups with associated metal cations). While they have many interesting properties, they have not developed into commercial products.

Given the importance and the impact on the global market of this class of materials, the thermoplastic elastomers, in the last twenty years academic research became interested in various field of TPEs worldwide.[2]

1.3 Classification and structure

The most accepted classification[1,7] want currently known TPEs divided in the following seven groups:

1. Styrenic block copolymers
2. Crystalline multi-block copolymers
3. Miscellaneous block-copolymers
4. Hard polymer/elastomer combination
5. Hard polymer/elastomer graft copolymers
6. Ionomers
7. Polymers with core shell morphologies

It is evident that with such a variety of materials it is to be expected that the properties of thermoplastic elastomers cover an exceptionally wide range. Some are very soft and rubbery while others are hard and tough, and in fact approach the ill-defined interface between elastomers and flexible thermoplastic.

More rationally classified classes, according to TPEs chemistry and morphology, were also presented:[2]

1. Block copolymers
    a. Styrenic block copolymers
    b. Thermoplastic copolyesters (COPE)
    c. Thermoplastic polyeurethanes (TPU)

d. Thermoplastic polyamides (COPA)

2. Blends and elastomeric alloys

a. Elastomeric rubber-plastic blends (TPO)

b. Thermoplastic vulcanizates (TPV)

c. Melt processable rubber

3. Ionomers

4. Miscellaneous

In this chapter, after a general analysis on the phase structure and the general properties of the thermoplastic elastomers, only TPEs based on polymer blends will be described in details, as they represent the central topic of this work, while the whole family of block copolymers, ionomers and miscellaneous thermoplastic elastomers will be presented in an overview.

1.3.1 Phase structure and characteristics

Thermoplastic elastomers demonstrate a number of unique properties as a result of their morphological features and have one feature in common: they generally exhibit a phase-separated system in bulk. (The only currently known exceptions are Alcryn®, a registered trademark of Advanced Polymer Alloys, that is a single-phase melt-processable rubber, and materials based on ionomers). One phase is hard and solid at room temperature whereas the other is an elastomer and fluid. Often the phases are chemically bonded by block or graft copolymerization. In other cases, for example in rubber/thermoplastic compositions, a fine dispersion of the phases is apparently sufficient to give the final material properties of thermoplastic elastomer. The properties of TPEs are strongly sensitive to which phases are present and how they are spatially

arranged (for instance, disperse versus co-continuous). Important parameters in this respect are crystallinity and crystals imperfection of the hard segment, composition of the amorphous phase, and continuity of different phases.

The hard phase gives these thermoplastic elastomers their strength. Without it, the elastomer phase would be free to flow under stress and the polymers would be unusable. When the hard phase is melted, or dissolved in a solvent, flow can take place and so the thermoplastic elastomer can be processed. On cooling or evaporation of the solvent, the hard phase solidifies and the thermoplastic elastomers regain their strength. Thus, in a sense, the hard phase in a thermoplastic elastomer acts similarly to the sulfur cross-links in conventional vulcanized rubbers and the process by which it does so is often called physical cross-linking. Conversely, the elastomer phase provides elasticity and flexibility to the system.

The individual polymers constituting the respective phases retain most of their characteristics, so that each phase exhibits its specific glass transition temperature (T_g) or crystalline melting temperature (T_m). These two temperatures determine the points at which a particular thermoplastic elastomer goes through transitions in its physical properties. An example of this is the measurement of the flexural modulus over a wide range of temperatures: as one can see in Figure 1.1, three distinct regions appear. At very low temperatures, both phases are hard and so the material is stiff and brittle. Above its T_g temperature the elastomeric phase becomes soft and the thermoplastic elastomer resemble a conventional vulcanizate. As the temperature is further increased, the modulus stays relatively constant (a region often described as the 'rubbery plateau') until finally, the hard phase softens. At this point, the thermoplastic elastomer becomes fluid. Thus, TPEs have two service temperatures, the lower service temperature depends on the T_g of the elastomer phase while the upper service temperature depends on the T_g (if amorphous) or the T_m (if crystalline) of the hard phase. The difference

between the upper and lower service temperatures is the service temperature range.

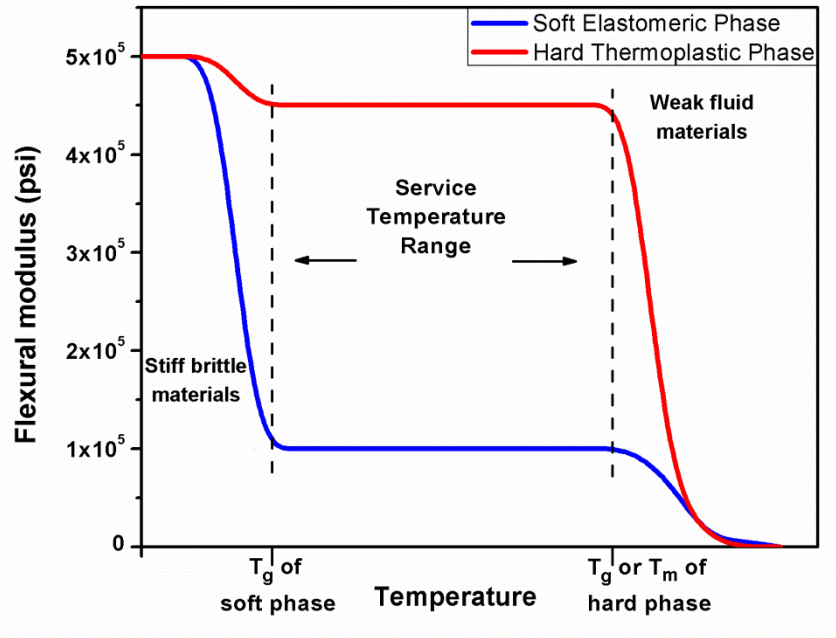

Figure 1.1: Stiffness of typical thermoplastic elastomers at various temperatures. The service temperature range is highlighted.

In addition to all the possible components for the two phases and the way they can be combined, the relative amounts of the hard and soft phases can be varied, as well. As might be expected, increasing the ratio of hard to soft phases lead to an exceptionally wide range of properties and applications for thermoplastic elastomers.

1.3.2 Thermodynamics of phase separation

Phases separation between components occurs since the dissimilar components, such as the homopolymers, are typically immiscible one with the other as a result of positive heat of mixing.

Anyway, in order to develop superior mechanical properties in a two-component polymeric system, the components should be neither so incompatible that they do not wet, nor so mutually soluble that would they form one homogeneous phase.[20] Most of the current known systems are compatible to the extent that a slight degree of mixing takes place or interfacial bonding is developed directly. This happens in graft and blocks copolymers and also in compatibilized polymer blends. Moreover, this could also happen in binary blends of two very different polymers that may have reactive sites along the chains that can react and form some kind of bonds or interactions: this will be revealed the case of the systems studied in the present thesis work.

Polymer incompatibility arises from the very small entropy gained by mixing different kinds of long chains. In fact, in the limit of high molecular weight, only polymer pairs with zero or negative heats of mixing form one phase.

Generally, materials mix to form a single-phase system if the free energy of mixing (ΔG_m) is favorable, that is, negative. This free energy can be expressed in terms of enthalpy of mixing (ΔH_m) and entropy of mixing (ΔS_m):

$$\Delta G_m = \Delta H_m - T\Delta S_m,$$

where T is the absolute temperature. The condition for domain formation (i.e., phase separation) is a positive value of the free energy of mixing. Thus,

$$\Delta H_m > T\Delta S_m.$$

ΔH_m is almost always positive for hydrocarbon polymers, because there are no strongly interacting groups, and it increases as the structure of the two polymers

forming the segments becomes less alike.[21] T and ΔS_m will always be positive and therefore the term $-T\Delta S_m$ will always be negative. However, this term will approach zero as the molecular weights of the segments become large and/or as the temperature decreases. Thus, we can expect domain formation to be favored by the following factors: segments with highly different structure; segments with high molecular weight; and low temperature.

There is a fundamental difference between phase separation in a system of incompatible homopolymers and that in a corresponding block copolymer system. In the latter, the two incompatible components are chemically bonded to one another (as will be explained more clearly below) and hence the segregated phases are restricted from growing indefinitely in size. So, unlike polymer blends where the constituting polymers separate at macroscopic scale, for block copolymers, only micro-homogeneous scale separation is possible, due to the covalent bond linking the blocks of different polymers, which forces them to regroup in smaller domains. The reasons for demixing of two blocks of the copolymer are the same as those for demixing of low molecular weight liquids.

The two or more distinct and incompatible moieties provide unique solid state and solution properties to block copolymers, which in turn lead to various applications.

Most theories take into account four factors that influence the phase separation of block copolymers: the Flory-Huggins interaction parameter χ, the overall degree of polymerization N, architectural constrains, and weight fraction of one component. By controlling appropriately the segment nature and length of each constituent of the blocks in block copolymers, a wide variety of microdomain structures of high degree of richness and complexity in bulk as well in solution phase are possible.[22] Their complex structure has significant effect on the static, dynamic and other functional properties of the final thermoplastic elastomer.

Microdomain structure is a consequence of microphase separation. It is associated with processability and performances of block copolymers as thermoplastic elastomers. The size of the domain decreases as the temperature increases.[23] At processing temperature they are in a disordered state, melt viscosity becomes low with great advantage in processability. At service temperature, they are in ordered state and the dispersed domain of plastic blocks acts as reinforcing filler for the matrix polymer.[24] This transition is a thermodynamic transition and is controlled by counterbalanced physical factors, e.g., energetic and entropy.

1.3.3 Surface and interface

The presence of two phases in TPEs influences its applications sensitive to surface or interfacial properties. The interphase between the hard and the soft portion is often considered as a separate phase and it can be substantially different from the bulk of the material. The presence of interface introduces thermodynamic factors that can alter the morphology near the interphase. The understanding of the influence of the interface on the properties of thermoplastic elastomers still needs in depth investigations, although it is well known that many stress-relieving processes, for example deflection and bifurcation of crack and sharing of loads or stress transfer, occur at the interface. At the interface between glassy and rubbery phases, some degrees of interpenetration of the constitutive blocks occur in the case of diblock systems.[25] Thus, lower the difference in solubility parameter, the higher will be the thickness of the interface where bonds between two types of blocks are generally found.

The adhesion between the interface and the polymer matrix is very important in the case of rubber plastic blends as often the failure occurs in such blends because of poor interfacial adhesion. Systems that have narrow interface usually show complete phase separation (i.e., more than the microscale). The important

parameter that characterizes the interfacial behavior of a material is the surface energy. It can be estimated from contact angle measurements of various liquids on given polymer surface.[26] The difference in the surface tension between elastomers and plastics, called surface energy mismatch, gives an estimation of interfacial tension between them during melt mixing. Interfacial tension determines the size of one phase dispersed in the matrix: lower mismatch gives finer dispersion.

Various adhesion tests have been performed and reported in the literature,[27,28,29] however, in the present thesis work, more sophisticated techniques will be presented for the analysis of the interfacial interactions in a binary rubber/thermoplastic blend obtained without the need of any particular compatibilizer.

1.4 General characteristics of TPEs

1.4.1 Advantages and disadvantages

Given the principles of how a thermoplastic elastomer works, it is clear that this class of materials offer a variety of advantages over conventional thermoset (vulcanized) rubber materials, which can be summarized in several points:

1. Simpler processing with fewer steps since TPEs use the processing method for thermoplastics, which are typically more efficient and significantly less costly. So the final cost of the finished part is lower.

2. Shorter fabrication times, which also lead to lower finished part costs. Since molding cycles for TPEs are typically several seconds as opposed to minutes for thermoset rubber, the productivity of the given equipment is greatly increased.

3. There is little or no compounding. The majority of TPEs is supplied fully formulated and ready for fabrication.

4. No vulcanization is required (except thermoplastic vulcanizates (TPVs) that will be further investigated), this allows to avoid one step in the process and in addition permits the avoiding to use generally dangerous and polluting chemicals.

5. The possibility of reusing scrap in the same fashion as with thermoplastics. The scrap from thermoset rubbers is very often discarded. Its amount generated may be in some cases comparable to the weight of the molded part. The TPE scrap can be reused as a regrind frequently, producing materials having the same properties as the virgin material.

6. Lower energy consumption due to shorter molding cycles and simpler processing.

7. Better quality control and closer tolerances of finished parts due to simpler formulation and process.

8. Lower quality control costs because of greater reproducibility and consistency of properties of TPEs.

9. Since most TPEs have lower density than conventional rubber compounds, their volume cost is often lower.

10. Properties can be easily manipulated by changing the ratio of the components (hard to soft). This is especially true, or at least generally easier and cheaper, for simple blends, compared to block copolymers that need new synthetic routes.

Of course there are also some disadvantages associated to thermoplastic elastomers if they are compared to conventional rubber materials. They include for example the softening and melting at elevated temperatures. This inherent

property limits the use of parts from TPEs to service temperatures well below their melting point. A thermoset rubber would be probably suitable for a brief exposure to that temperature. From this reason (the absence of a true chemical cross-link) arises also another disadvantage: these materials show creep behavior on extended use.

Other negative points on TPEs, concerning the general properties and the processing properties respectively, are the limited number of low hardness TPEs and the needs to drying prior to processing (this step is almost never used for conventional rubber materials but is quite common in fabrication of thermoplastic in general).

1.4.2 Factors influencing the properties

Since TPEs typically consist of two immiscible phases at service temperature, the final properties of TPEs are influenced by the properties of the individual phases and the interface. It is therefore necessary to consider several factors to understand the final properties of thermoplastic elastomers.

The constituents of the TPEs clearly play a vital role in determining the properties. In triblock ABA-type styrenic copolymers, the change in the center-block or the end-block results in difference in properties: despite the fact that the T_g changes with the type of center elastomeric block, no marked effects due to this difference is observed at room temperature; However, substitution of α-methyl styrene gives rise to a tougher polymer that is partially due to higher T_g values of this block. This emphasizes the major role of the hard phase on the mechanical properties of TPEs.[2]

For the other block copolymers (thermoplastic urethanes (TPU), copolyamides (COPA) and copolyesters (COPE)) and also for polymer blends, changing hard segment (or hard moiety) type will affect the crystallinity of the

hard phase. In TPUs, symmetric diisocyanates produce strong TPEs, whereas substituent on the aromatic ring tend to reduce the mechanical properties.[30]

The soft segment type may instead influence the driving force for phase separation and hence the mechanical properties. Furthermore, it has been observed that soft segments, which are capable of strain crystallizing, produce a tough material with higher tensile strength and tear resistance.

The molecular weight is also a factor that influences a lot the properties of the TPEs, both deriving from block copolymers and from polymer blends. For the latter, also the molecular weight distribution is important in determining the miscibility/phase separation length scale and thus the final mechanical properties. In block copolymers, increasing the M_w of the soft segment promotes phase separation, which will reduce the fractional conversion. The effect of hard segment block length is also important: the longer blocks lead to phase separation and better properties.[31]

The relative proportion of hard and soft segments is another important factor that decides whether the elastic properties of a TPE would be more close to those of a cross-linked elastomer or of hard plastic, and this will be especially discussed and demonstrated in this thesis work.

The material changes from a flexible elastic rubber to semi-rigid plastic with increasing hard segment content, and at a very high level of the hard segments the material behave more like toughened plastic. Therefore, TPE features are obtained within certain composition range of the components.

In case of multiblock-segmented block copolymers (like TPU, COPA and COPE) the performance characteristics of TPE depend on the weight fraction of crystallinity of hard phase and its T_m.[32] Crystallinity affords a mean for rather large deformation in the hard phase. Like presented before, the useful temperature range for a TPE is between T_m and T_g. Within this range a TPE is

elastomeric, below which it is brittle and above which the hard phase melts (passage from T_g to T_m is reversible) and the elastic properties of a TPE blend, for example Young and shear moduli, are functions of elastic properties of the components. Strength of the hard phase represents limit for strength of such blend, even thou the elastic modulus may result enhanced by interface adhesion effects.[33]

The conditions applied during processing and fabrication of TPEs will be the last effect cited here that strongly influence their morphological features and hence their final properties. When producing samples of polymer blends, for example by injection molding, if the shear strains applied are hard enough, the domain structure is fine textured, and an isotropic article will be produced. If non-directional shear strains are frozen into the material, the material will be isotropic.

1.4.3 General properties of Thermoplastic Elastomers

The majority of TPEs function as a rubber until temperatures as low as -40 °C or even lower as measured by their brittle point. The upper temperature limit is determined by the maximum temperature at which it can give satisfactory retention of tensile stress-strain and hardness properties. The upper service temperature increases with cost.

Styrenic with saturated soft block (SEBS, see next paragraph 1.5) have higher heat resistance than those with diene soft blocks. Elastomeric alloys from saturated elastomer also give better high temperature performance characteristics than those from an unsaturated elastomer backbone.

TPEs generally extend to high elongation and often in some cases with residual elongation or permanent set. Their set properties are in between elastomers and thermoplastic. Sometimes stress softening and strain hardening in

elastomeric alloys can occur, a model proposed in the literature explains that strain hardening is a result of interaction of rigid thermoplastic domain.[34]

In TPE, the hard domains can act both as filler and intramolecular tie points; thus, the toughness results from the inhibition of catastrophic failure from slow crack growth. Hard domains are effective fillers above a volume fraction of 0.2 and a size larger than 100 nm.[35] The fracture energy of TPE is characteristic of the materials and independent of the test methods as observed from rubbers. It is, however, not a single-valued property and depends on the rate of tearing and test temperature.[36] The stress-strain properties of most thermoplastic elastomers have been described by the empirical Mooney-Rivlin equation:

$$\sigma = (\rho RT/M_c + 2C_2/\lambda) \cdot (\lambda - 1/\lambda^2)$$

where σ is the stress, ρ is the density of the system, R is the gas constant (8.314 $J \cdot K^{-1} \cdot mol^{-1}$), T is the temperature, M_c the molecular weight between cross-links and λ is the extension ratio. C_2 is just an experimental constant.

When plastic portion act as a physical cross-link and strength properties are indirectly related to the modulus of hard phase and morphology of the blend, the hard part's filler effect is analyzed by the following equation:

$$E_F/E = (1 + 2.5\phi + 14.1\phi^2)$$

where E_F/E is the ratio between the modulus of the filler/the modulus of unfilled elastomer and ϕ is the volume fraction of the filler.

The typical tensile behavior of TPE with change in temperature is well represented by single parabolic curve: as the temperature rises in TPE, modulus and strength decrease due to the softening of hard domain, in the vicinity of softening point, the properties decrease dramatically and the material cannot be used as a thermoplastic elastomer.[37]

Most of the TPEs are in the high rubber-hardness range (above 80 Shore A), that was cited as a lack in the wide range of TPEs properties. In general, a thermoplastic elastomer will be less rubbery and more like a thermoplastic as hardness is increased, and the compression set resistance at ambient temperature will decrease with increase in hardness, as expected.

The resistance of a TPE to different chemicals is influenced greatly by its chemical similarity to the fluid. For example, the non-polar styrenic and thermoplastic olefins have high resistance to polar chemical, while the polar TPU, COPA and COPE have better resistance to hydrocarbon fluids, but poorer resistance to polar chemicals than that of conventional rubbers.

TPEs are also very susceptible to oxidation at elevated temperature. Antioxidant and other additives could improve the chemical resistance of these materials, even thou, should be better to avoid this and to choose the soft portion to be intrinsically resistant to oxidation, e.g., non-dienic rubbers.

The melt rheological behaviors of TPEs are strongly dependent on shear rate, temperature and composition. TPEs exhibit wide variation in viscosity and elasticity; a wide variation in morphology results in semi-Newtonian to highly shear-thinning behaviors. There are fundamental differences in rheological responses between a conventional rubber and a TPE: in the vicinity of the T_g of the soft segments, in TPEs, both phases are very resistant to stress and below this temperature they behave as a single-phase brittle glassy polymer. On increasing temperature, the hard domain starts weakening and flows. The melt rheology of TPEs is thus related to that of hard segment and/or plastic materials.

TPE viscosity is less sensitive to temperature than shear rate, indicating the fact that input of mechanical energy is more effective during processing than the input of thermal energy. In an injection molding operation, higher injection pressure will have a significant impact on flow rate and fill time than a change in temperature.

1.5 TPEs based on block copolymers

In the following section, a brief introduction to the most known thermoplastic elastomers that appertain to the family of block copolymers will be given. Common preparation and general characteristics and applications of these materials will be concisely discussed, especially for those that are well-known commercially available polymers.

1.5.1 Styrenic block copolymers

Styrenic block copolymers are based on simple molecules such as an S-*E*-S block copolymer, where S is a polystyrene segment and *E* is an elastomer segment. The two segment types are incompatible and so form a two-phase system. The most common are those for which the elastomer segment is a hydrocarbon, most likely polyisoprene or polybutadiene.

Two basic polymerization systems, anionic[38] and carbocationic[39] are used to produce these styrenic block copolymers. However, the products share many common features that can be considered together.

If the elastomer is the major constituent, the block copolymers should have a morphology similar to that shown in Figure 1.2:

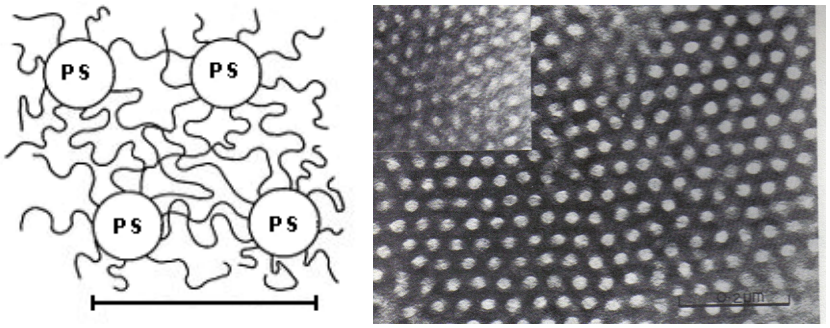

Figure 1.2: Schematic representation of the morphology of styrenic block copolymers (left). The scale bar represent the phase separation length scale between the PS hard domain and the elastomeric soft and amorphous phase, and it is in the range of 100-200 nm. On the right: transmission electron micrograph of an S-*E*-S block copolymer, the elastomeric phase is stained black. Scale bar: 200 nm.

Here, the polystyrene end segments form separate regions, i.e., domains, dispersed in a continuous elastomer phase. Most of the polymer molecules have their polystyrene end segments in different domains. At room temperature, these polystyrene domains are hard and act as physical cross-links, tying the elastomeric mid-segments together in a three-dimensional network. In some ways, this is similar to the network formed by vulcanizing conventional rubbers using sulfur cross-links. The difference is that in thermoplastic elastomers the domains lose their strength when the material is heated or dissolved in solvents. This allows the polymer or its solution to flow. When the material is cooled or the solvent is evaporated, the domains harden and the network regains its original integrity.

This domain theory explains what at first seemed very particular properties. Moreover, a direct evidence of the microstructure of such materials has been

given since many electron micrographs were published, some showing a remarkably well defined and regular structure.[40]

In addition, in these materials block copolymers, the elastomeric chains are highly entangled, and many of the critical strength properties derive from these entanglements.[4] As well as functioning as cross-links, the hard domains prevent these entanglements from disentangling under stress.

It should be noted that analogous block copolymers with only one hard segment (e.g., S-*E* diblock or *E*-S-*E* triblock copolymers) have quite different properties.[4] In these polymers the soft phase cannot form a continuous interlinked network because only one end of each elastomer segment is chemically bonded to the hard domains. These polymers are not thermoplastic elastomers, but are weaker materials similar to unvulcanized synthetic rubbers.

In addition, the hard polystyrene domains act as reinforcing fillers for the material. Effective reinforcing fillers used in the rubber industry (to improve the physical properties) such as carbon black are hard, small, well-dispersed particles that are strongly bonded to the elastomer chains and prevent small stress-induced cracks in the elastomer for spreading and initiating catastrophic rupture. The hard polystyrene domains in S-*E*-S block copolymers fulfill all these requirements: they are small (<300 Angstroms in diameter) and obviously well dispersed. In addition they are strongly bonded to the elastomeric phase because they are part of the same molecule.

As in other thermoplastic elastomers, the morphology of these styrenic block copolymers depends on the ratio of the volume of the hard polystyrene phase. This ratio can be varied within quite wide limits. In the general case,[41] in a block copolymer of *A* and *B*, as the ratio of the *A* to *B* segments is increased, the phase morphology changes from a dispersion of spheres of *A* in a continuous phase of *B*, to a dispersion of rods of *A* in a continuous phase of *B*. Further increases in the ratio of the *A* to *B* segments yields a lamellar or “sandwich” structure in which

both *A* and *B* are continuous. If the proportion of *A* is increased still further the effect is reversed; *A* now becomes continuous and *B* dispersed (see Figure 1.3).

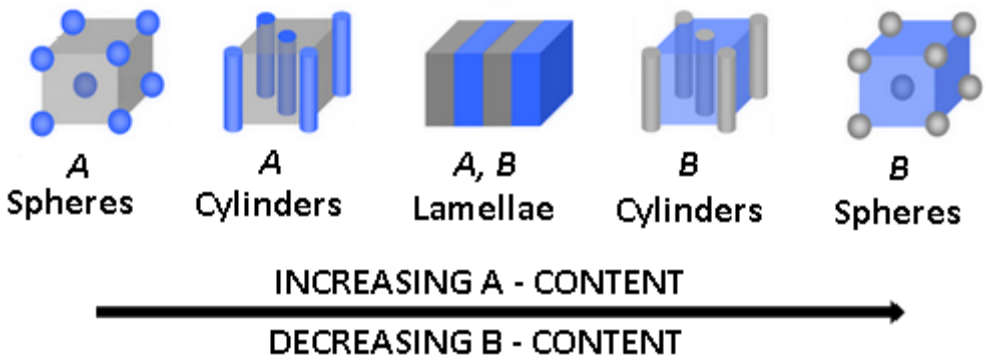

Figure 1.3: Changes in morphology with composition in *A*-*B*-*A* block copolymers. *A* phase is represented in blue and *B* phase is represented in grey.

Because of this change in morphology, as the polystyrene content increases, the stress-strain behavior of the TPE changes from soft weak material to a strong elastomeric material and then, at about 45% polystyrene content, to a hard, leathery material with a yield point, in its stress-strain curve, typical of thermoplastics.

The balance between properties and processability for styrenic thermoplastic elastomers leads to focusing on unique applications in addition to the replacement of general-purpose rubber. Styrenic block copolymers are rarely used as neat polymers and can be readily mixed with other polymers, oil, and fillers, which allow versatile tuning of product properties.

Formulated styrenic thermoplastic elastomers have several major applications:

1. Replacement for vulcanized rubber;

2. Adhesives, sealant and coatings;

3. Bitumen modification;

4. Viscosity index improvers for lubricating oils;

5. Modifiers for thermosets.

In addition to those important applications, styrenic TPEs have met a large interest in the academic research, especially since Atomic Transfer Radical Polymerization (ATRP)[42] and Radical Addition-Fragmentation Reversible polymerization (RAFT)[43] have been developed and have permitted to obtain many new morphologies for this family of thermoplastic elastomers.[44,45]

1.5.2 Multi block copolymers

These polymers have more complex structure than the styrenic block copolymers. They are based on multi-block $(H\text{-}E)_n$ copolymers in which the hard (*H*) segments are often crystalline thermoplastics, while the softer (*E*) segments are amorphous and elastomerics.[1]

It is a general principle that crystalline polymers (or segments) must have a regular repeating structure along the polymer chain. Polymers that do not have this regular repeating structure cannot crystallize and so, are amorphous.

The resultant multi-block $(H\text{-}E)_n$ polymers have a morphology similar to that shown in Figure 1.4.

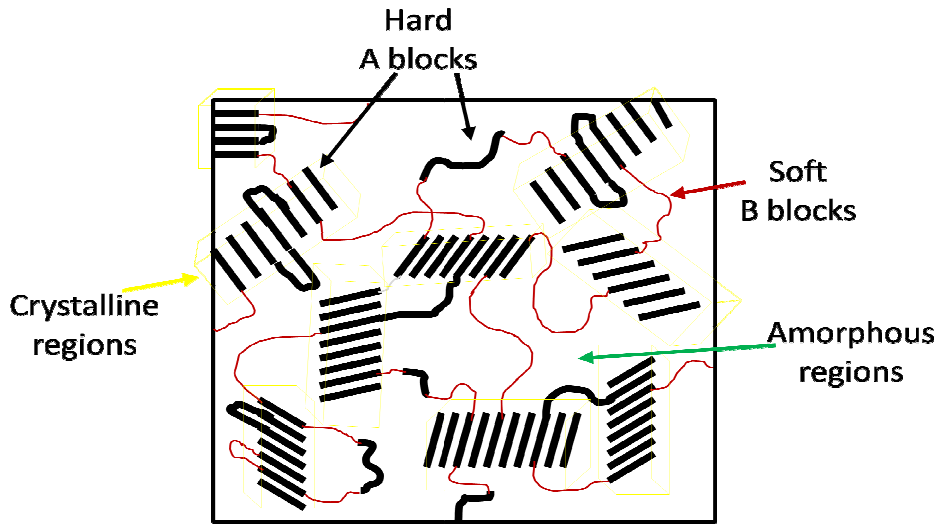

Figure 1.4: Schematic representation of the morphology of multiblocks polymers. hard segments are arranged in a crystalline phase.

Here, the hard crystalline segments form an interconnected structure interspersed with the elastomeric phase. A single molecule can traverse several crystalline regions. Depending on the quality of the crystallization process, some hard segment material may lay in the elastomeric phase and may not crystallize. However, most of the hard segment material forms in separate regions. At room temperature, these crystallize and act as physical cross-links, tying the elastomeric mid-segments together in a three-dimensional network. In some ways, this is similar to the network formed by the styrenic block copolymers. In both cases, the hard regions loses their strength when the material is heated, allowing the polymer to flow. When the material cools, these regions become hard again and the network regains its original integrity.

The principal families of multi-block copolymers are thermoplastic polyurethanes (TPU), thermoplastic polyamides (COPA) and polyester thermoplastic elastomers (COPE); and they will be hereby briefly introduced.

Thermoplastic polyurethanes (TPU) are block copolymers obtained from the reaction of a low-molecular mass glycol chain extender (i.e., a macroglycol) with a diisocyanate. The basic chemical reaction in making any type of polyurethane including TPU is the urethane group formation. This is almost always accomplished by reaction of an organic isocyanate (–N=C=O) with an alcoholic hydroxyl group (–OH). The polymerization is carried out by a two-step process or a one step process. The former involves the preparation of a low molecular mass, isocyanate-terminated prepolymer followed by its chain extension to a high molecular weight polymer. The properties of thermoplastic polyurethanes depend on the nature of the phase structure. In general, they have excellent abrasion resistance and toughness, and they posses also good oil resistance, in addition to high strength, tear resistance, low temperature flexibility and resistance to attack by fungi and bacteria. For these reasons, TPUs find applications in demanding areas such as automotive, sporting and mechanical goods, fabric coatings and biomedical applications.[7]

Thermoplastic polyamides elastomers (COPA) consist of a regular linear chain of rigid polyamide segments interspaced with flexible polyether segments. They are basically segmented block copolymers having general structure $(AB)_n$. The hard segments may be based on partially aromatic polyamide or aliphatic polyamide. In these copolymers, the soft segment of aliphatic polyesters is linked to the hard segment by an ester group. The three principal methods for preparing COPA are the following: I. The formation of an acid-terminated soft segment, followed by the reaction of a diisocyanate and additional diacid to form polyester amide; II. The formation of an adipic acid-capped hard segment block of poly(11-aminoundecanoic)acid, joined with a soft segment of polyol in a polyesterification process; III. A process without ester linkage: the bonds between the two segments are amides.

Again the properties depend on the type of building blocks used. In general, because their high service temperatures, good thermal aging, and chemical resistance, COPA are the primary candidates for automotive under-the-hood applications and for high-temperature insulation of wires and cables.[7] Their high impact strength, tear, abrasion, low temperature and flex fatigue resistance open a great variety of applications in hose and tubing, seals and gaskets, bellows and other molded technical goods.[7]

Polyester thermoplastic elastomers (COPE) are segmented copolyether esters formed by the melt transesterification of dymethyl terephthalate, a polyalkylene ether diol and a low molecular mass diol. The long hard segments crystallizable of tetramethylene terephthalate act as cross-links that bind the soft amorphous polyalkylene ether glycol terephthalate into a network and thus the whole system behaves like conventional cross-linked elastomer.

Continuous and interpenetrating crystalline and amorphous regions exist in these materials. Although a two-phase structure was supported by electron microscopic and X-ray diffraction data, low-angle light scattering patterns conform to a spherulitic morphology.[5] The hard block crystallizes into a lamellar structure that forms the skeleton of the spherulitic structure.

The COPEs have better tensile properties at higher temperatures, lower compression set and better chemical resistance compared with TPU of equal hardness.

In commercial applications, COPEs can replace a variety of conventional materials, such as metal, cast polyurethane, leather, and rubber. Within their elastic design range, COPEs offer two to fifteen times the strength of vulcanized rubber. Because of that, it is common to redesign rubber parts for one half to one-

sixth the original part thickness and weight. Non-reinforced COPEs also can replace composites of rubber with metal, fibers and fabric.

1.5.3 Other Thermoplastic Elastomers

Previous paragraph dealt in some detail with the types of thermoplastic elastomers that have become commercially important. Naturally, these are the ones that attract most attention. However there are other potential routes to achieve these properties and a couple will be briefly described here as examples: graft copolymers, and ionomers.[1]

The generalized structure for a graft copolymer is represented as:

$$E\text{-}\ldots\text{-}E\text{-}E\text{-}\left(\begin{array}{c}\text{-}E\text{-}\\ |\\ H\end{array}\right)_n\text{-}E\text{-}\ldots\text{-}E\text{-}$$

This represents a polymer where each elastomeric poly *E* backbone chain has (on average) *n* random grafts (covalently bonded) of pendant hard *H* segments. If the molecular weight of the hard segments is sufficiently high, they phase separate and form an interconnected network similar to that formed by the physical cross-linking of linear styrenic triblock copolymers.

The molecular weight of these pendant *H* groups that attach to each elastomer molecule is a statistical distribution; in other words, one can only speak of the average number *n* of pendant groups per elastomer molecule. For satisfactory properties, *n* must be at least 4. Thus, if the hard segment molecular weights and proportions are the same, a graft copolymer with $n = 4$ would have twice the molecular weight of the corresponding *H-E-H* triblock copolymer. For this

reason, at equal hard segment molecular weights, graft copolymers have higher viscosities than equivalent triblock copolymers, which should make them more difficult to process.

However, the potential to use pre-polymerized elastomer chains is an advantage: these elastomer can be resistant to degradation. The T_g of the hard segments can be very high; alternatively crystalline polymers can be used.

Graft copolymers usually have lower strength properties than block copolymers, and for this reason they are mainly used blended with the corresponding triblock copolymer in order to reduce the strength of the final properties for some niche applications.

An example of the structure of an ionomer that behave like thermoplastic elastomers may be given from the following molecule:

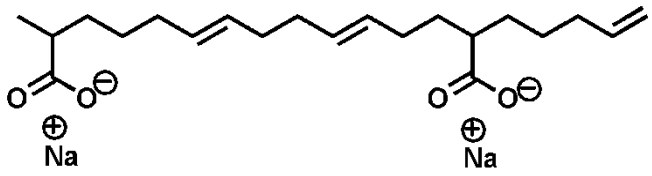

This represent an elastomer molecule that has carboxylates groups (COO^-) polymerized into the backbone chain; and these are neutralized by metallic counterions (Na^+). These counterions associate together to form ionic clusters that can behave like the hard polymer domains in block and graft copolymers; in other words they tie the elastomer chains together in a physically cross-linked network. This system gives flexible rather than elastomeric products because the backbone chain is mainly polyethylene. Replacement of the polyethylene by an elastomeric polymer is an obvious extension. Many different acidic groups have been investigated, including carboxylates and sulfonates.[46]

Thermoplastic elastomers with hardness as low as 70 Shore A can be produced,[47] but have not been commercialized.

1.6 Hard polymer / elastomer combination

There are two types of these materials: simple blends of the two polymers (the hard thermoplastic and the soft elastomer) and dynamically vulcanized products in which the elastomer is cross-linked during the mixing process.[1]

The first useful rubber/plastic blends were those obtained from nitrile rubber (NBR) and polyvinyl chloride (PVC); since that moment, those kind of blends have gained considerable interest for the development of new materials and there have been constant researchers going on in this field. The main reason is that both the hard polymers and the elastomers used to make these products can be obtained very easily without the need of new synthetic processes. Thus, an extremely wide range of combinations can be investigated quickly and easily. Similarly, commercial products can be made without the very high capital investment usually required to produce new polymers.

1.6.1 Simple blends

Most simple blends are produced by mixing the hard polymer and the elastomer together on high shear compounding equipment.

Polymer blends can be broadly divided into three categories, according to the IUPAC Gold Book,[48] and the following nomenclature will be used within all this thesis work:

1. Immiscible polymer blends (heterogeneous polymer blends): This is by far the most populous group. If the blend is made of two polymers, two glass transition temperatures will be observed.

2. Compatible polymer blends: Immiscible polymer blend that exhibits macroscopically uniform physical properties. The macroscopically uniform properties are usually caused by sufficiently strong interactions between the component polymers. Two different glass transition temperatures will again be observed, but with deviation caused by the presence of the over mentioned interactions between the phases.

3. Miscible polymer blends (homogeneous polymer blend): Polymer blend that is a single-phase structure. In this case, one glass transition temperature will be observed.

Thermoplastic elastomers are, by definition, phase separated systems, thus, only the first two categories can give rise to materials with TPEs properties.

Many possible morphologies can be formed in a two-phase system, for the purpose of this section, hard polymer/elastomer blends will be referred to have one of the following three structures:

1. A dispersion of the elastomer in a continuous phase of the hard polymer. Here the stiffness and strength of the hard polymer predominate. The result is a flexible and tough thermoplastic, characterized by an yield point in its stress-stain curve and differing from a pure plastic mainly concerning the improved impact properties.

2. A dispersion of the hard polymer in a continuous phase of the pure elastomer. Here the stiffness and strength of the elastomer phase predominate. The result is essentially a filled, unvulcanized elastomer, in which the dispersed

particles of the hard thermoplastic polymer act as the filler. Because the elastomer is unvulcanized, it has little strength and the product is soft but too weak for practical applications.

3. A three-dimensional, continuous and interpenetrating (co-continuous) structure of the hard polymer and the elastomer. This structure can be visualized as similar to an open cell foam (or, most simply, to a sponge), in which the foamed material (or the sponge animal) is one phase and the air is the other. A two-dimensional representation is depicted in Figure 1.5. This structure yields a product with strength derived from the continuous hard phase and the flexibility derived from the continuous soft phase. Because neither phase is cross-linked, both can flow and the result is a thermoplastic elastomer.

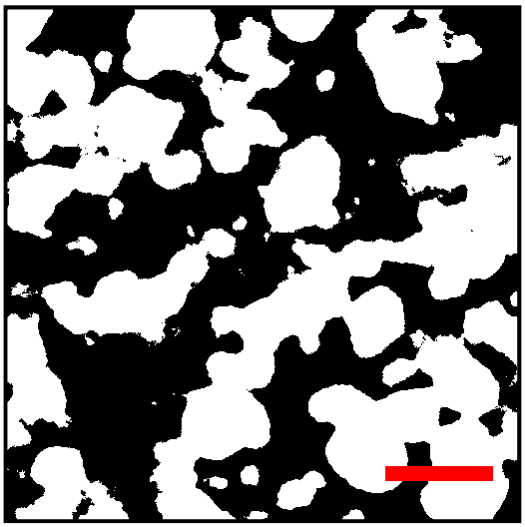

Figure 1.5: Bi-dimensional representation of a typical co-continuous morphology of a hard polymer/elastomer blend. Scale bar represents the phase separation length scale, that in TPE blends normally ranges from 1-2 microns to 10 and more microns.

The structure described in the third point is critical for the formation of a thermoplastic elastomer from a simple two-component blend. There are several requirements for this formation.

The most important is that the viscosities of the two polymers must be matched at the temperature and shear rates of mixing. The temperature during mixing can be controlled by adjusting the heating systems on the mixing equipment. The shear rate is in the range of 100 to 1000 sec^{-1}, with the lower end of this range being typical of rubber processing equipment, such as Banbury internal mixers and rubber mills. Conversely, the upper end of this range is typical of plastic processing equipment, such as twin screw extruders. The optimum viscosity match also depends on the proportions of the two components. This approach predicts that an ideal viscosity match exist when:[49]

$$Log_{10}(\eta_A/\eta_B) = 2 - 4\phi_B$$

where η_A and η_B are the viscosities of the components *A* and *B* at the processing conditions and ϕ_B is the volume fraction of the component *B*.

Other workers[50] have used the expression

$$\eta_A/\eta_B = \phi_A/\phi_B$$

As a criterion of ideal mixing.

In practice, these two expressions give similar results unless the volumes of the two components are very different. Both predict that if the volume of the two components are about equal, then for ideal mixing, their viscosities should also be about equal. If the volume are not equal, then the component with the larger volume should also have the higher viscosity. Increasing the ratio of the viscosities to well above the optimum range favors the formation of a dispersed phase of the lower viscosity component.

The other important factor that affect the formation of co-continuous phases is the compatibility of the two components, which is often judged by the difference between their solubility parameters. This difference can be correlated with the interfacial tension between the two polymers. If two polymers (or more generally, two immiscible liquids) have a large interfacial tension, the formation of a two-phase system with large phase dimensions (i.e., a coarse dispersion with a large phase separation length scale) is favored. This coarse dispersion reduce the interfacial area and hence, the interfacial energy. In contrast, polymer pairs with similar solubility parameters tend to form a finer dispersion.[49] Thus, if the two polymers have different solubility parameters, i.e., one is polar while the other is hydrophobic, they will probably form a coarse dispersion with poor adhesion between the phases.

The time mixing is also often a determinant of particle size and shape: sometimes morphological changes after mixing occur by simply coarsening of rubber-plastic emulsion due to melt agglomeration.[49]

More specific description of co-continuous phases formation in polymer blends will be given in section number 1.6.3.

1.6.1.1 Examples of Thermoplastic Elastomers from rubber/plastic binary blends

The most commercially significant TPEs obtained by mixing a rubber and a plastic are those based on polypropylene (PP).[51] PP has the advantage of being low in both cost and density. Additionally, its crystalline structure and relatively high crystal melting point give it resistance to oil, solvents, and high temperatures. Ethylene-propylene (EPM) or ethylene-propylene-diene (EPDM) rubbers are the obvious choices for the corresponding elastomeric phase because of their thermal stability, low cost, low temperature flexibility, and structural

similarity to (and hence, technical compatibility with) polypropylene. Thus, well dispersed blends of PP with EPM or EPDM rubbers are low cost, easy to make, and have a wide service temperature range.

An entirely different class of thermoplastic elastomers is based on blends of polyvinyl chloride (PVC) as the hard phase with nitrile rubber (NBR) and a plasticizer, often dioctyl phthalate (DOP) and more recently diisononyl phthalate (DINP). This technology has been known for more than 60 years[52] and is an extension of the even older technology to produce plasticized PVC.[53] These blends are at the ill-defined interface between flexible thermoplastic and thermoplastic elastomers. The acrylonitrile content of the NBR, its molecular weigh, and its degree of branching can be varied to suit the end use requirements.[5]

The blending of natural rubber (NR) with a thermoplastic material give rise to a class of TPEs from rubber/plastic blends known as thermoplastic natural rubbers (TPNR).[54] The development of TPNR was principally based on the criteria set by EPDM blends with thermoplastics. Blends of NR with polyethylene (PE) and blends of NR with polypropylene (PP) are the most studied and developed TPNR within the years.[54] TPNR is normally prepared via mixing in a Banbury mixer or a Brabender Plasticorder attached with a mixer or a twin screw compounder. Their properties, as usual, depends widely on the ratio between the components and their characteristics.

Aside those three important examples of TPEs polymer blends, many others rubber plastic blends are reported to exhibit thermoplastic elastomeric behavior and some have been commercialized. Section 1.6.4 of this chapter will be entirely dedicated to the description of Nylon-rubber blends, as they represent the main topic of this thesis work.

Other well-known examples of miscellaneous plastic/rubber blends are polyethylene-silicon rubber blends, polyethylene-butyl rubber (PE-IIR) blends,

polypropylene-nitrile rubber (PP-NBR) blends, polyethylene-ethylenevinyl acetate (PE-EVA) blends, polypropylene-ethylenevinyl acetate (PP-EVA) blends, and blends of polystyrene with various rubber such as IIR, EPDM, NR, styrene-butadiene rubber (SBR), chloroprene rubber (CR), EVA or NBR.[5]

Lastly, also blends of commercial thermoplastic elastomers (styrenic, TPU, COPE, etc.) with other polymers show thermoplastic elastomeric behavior.[7] Moreover, blending of thermoplastic elastomers with other polymers has considerable practical importance from the point of view of economic factors as well as property modifications. In general, thermoplastic elastomers are quite costlier materials, compared to the "raw" common commercial polymers. These materials can be made cheaper by blending with other compatible polymers: for example, expensive thermoplastic elastomers like copolyesters and polyurethanes whose property spectrum is much higher than is needed for a particular application may be blended with cheaper materials so that the resulting polymer blend would have a cost/performance ratio that makes it attractive for the given utilization. The physical properties of these polymer blends are generally a compromise or superior to the properties of the individual constituent polymers.

1.6.2 Dynamic vulcanizates

Structure and properties of thermoplastic vulcanizates (TPVs) are quite different from the ones of simple rubber/plastic non-vulcanized blends.[1] In particular, the structure now consist of a fine dispersion of a cross-linked (i.e., vulcanized) elastomer phase in a matrix of hard thermoplastic (see morphology on the right in Figure 1.6). The unvulcanized elastomer, the vulcanizing agents, and the hard thermoplastic are all mixed together under high shear. The mixing temperature must be sufficient to melt the hard thermoplastic and at the same time to cause vulcanization. This takes place under high shear or "dynamic" conditions, in contrast to the static conditions of vulcanization in a typical rubber

mold. When the vulcanization starts, the viscosity of the elastomer phase increases dramatically, to the point where there is a viscosity mismatch between the elastomer phase and the hard phase, since the viscosity of this latter phase remains the same. This causes the elastomer phase to break up into a fine dispersion into the thermoplastic matrix, and vulcanization continues in this state. This process is schematically shown in Figure 1.6. Shear must be applied until vulcanization is complete, otherwise the rubber particle can agglomerate. Small particle size is critical in order to obtain satisfactory properties in TPVs: tensile properties highly improve as the particle size decreases.

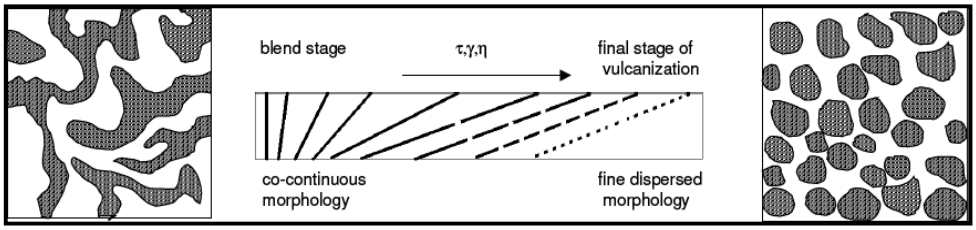

Figure 1.6: Schematic of the morphology evolution of a binary polymer blend during the process of dynamic vulcanization. Dark color represent the elastomeric phase. The parameters τ, γ and η are respectively the torque, the ratio between component and the viscosity.

The dynamically vulcanized thermoplastic elastomers have been the subject of much research and have had many applicative uses. In particular, Coran and Patel[11-19] have been analyzing in depth several important rubber plastic compositions, during the early eighties. These authors gave several criteria that must be met for the end product to have satisfactory properties:

1. The surface energies of the hard phase and the elastomer must match.

2. The molecular weight between inter-chain entanglements in the elastomer phase must be low.

3. Crystallinity must occur in the thermoplastic phase.

4. The elastomer phase must be able to be vulcanized at the mixing temperature.

5. Both phases must be thermally stable at the mixing temperature.

In addition of all these factors, the choice of vulcanizing agents is also important.

When compared to corresponding hard polymer/elastomer simple blends, dynamic vulcanizates have some significant advantages. For example, the amount of the elastomer in the total blend can be increased, anyhow avoiding the presence of a continuous soft elastomeric phase (note that the elastomer is vulcanized and finely dispersed in the thermoplastic matrix), thus softer products with however good physical properties can be obtained. In addition, being the soft phase chemically cross-linked, it cannot dissolve in solvents, oil or gasoline. For the same reason, contrary to an unvulcanized elastomer that flow when it is mechanically stressed, TPVs commonly show much less permanent set.

In any case, they have the obvious disadvantages that, even if the curing industrial step is avoided, the compounding with chemicals for the vulcanization is needed, and scraps cannot be recycled.

Concerning the commercial applications, because their wide spectrum of properties, they found applications in many areas such as automotive; hoses, tubes and sheets; mechanical rubber goods and consumer goods; architectural and construction; electrical and electronic; medical and food contact.[7]

1.6.3 Co-continuous structures in polymer blends

Co-continuous structures can be regarded as the coexistence of at least two continuous structures within the same volume, this means that both components have three-dimensional spatial continuity on some finite scale of mixing.[55] Co-continuous structures usually can be formed within a composition region about the phase inversion composition, which mainly depends on the viscosity ratio. The interfacial tension plays an important role for the stability: a lower interfacial tension leads to broader compositions ranges of co-continuity structures.[33] In a binary co-continuous blend, the surface of each phase is an exact topological replica of the other; as shown in Figure 1.7, they are antitropic, that is, complementarily reversed.

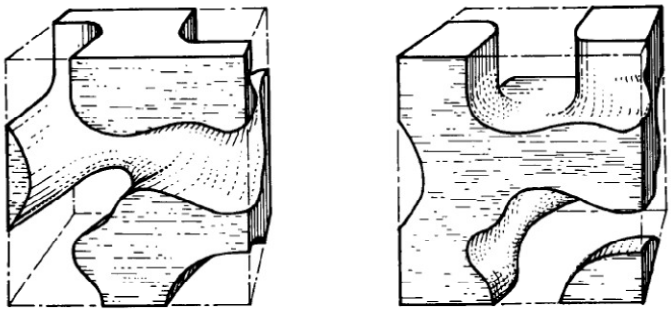

Figure 1.7: model of the antitropic structure of both components of a co-continuous blend. (Reproduced from Ref.[55]).

The structure obtained after mixing two immiscible polymers is determined by the rheological properties of the blend components, interfacial tension, blend composition and processing conditions. Although most commercial polymer blends have matrix-dispersed particle structures,[56] there is an increasing interest in co-continuous blends because this morphology type can offer some better

combinations of the component properties than are possible from dispersed-type structures.[57,58] For example, blends with co-continuous structures may combine the properties of both components in a favorable way (mechanical moduli, as an example) since the structure gives the maximum contribution from each component simultaneously,[59] synergistic effects on the macroscopic properties have also been shown in the literature.[60,61] To take advantage of such structures in materials produced by melt mixing, it is important to understand which processing conditions lead to their formation and especially the conditions for their stability.

As anticipated before, to develop co-continuous structures the most effective mixing can be achieved when the viscosities and the volume fractions of the two components are equal (equivolume-equiviscous mixing). This maximize the opportunity for maintaining connectivity because neither component is present in a minor amount. Nevertheless, in most system the viscosity of the components are different. The low-viscosity phase tends to be continuous because this minimizes energy dissipation in the flow field. To compensate for this tendency, the volume fraction of the higher-viscosity component has to be increased to the same extent as the viscosities differ to maintain the connectivity between the phases. In a quiescent melt, a co-continuous structure will be transient because the interfacial tension between the incompatible polymer components drives the system toward a minimum surface free energy. This will result in breakup of the co-continuity and lead to phase domain growth. Only when the network structure is kinetically inhibited from breakup and retraction the co-continuous structure can be preserved. For the formation of stable co-continuous structure the literature discusses two different mechanisms:[55]

1. coalescence of preformed dispersed particles to networks. As the content of dispersed phases increases, coalescence increases dramatically, leading to larger

particle sizes; simultaneously, at certain compositions, co-continuous structures are formed.

2. Sheet formation mechanism followed by sheet breakup to a network with extended structures. For immiscible but compatible binary blend systems exhibiting low interfacial tension, the continuity development and the microstructural features are consistent with a mechanism dominated by thread-thread coalescence; however, immiscible blends with high interfacial tension attain a co-continuity through droplet-droplet coalescence. Anyhow, the stability of co-continuous structures is governed by some of the same factors influencing their formation, as like as the interfacial tension/interactions, viscosities of the phases and composition ratios. For practical applications, however, the essential requirement is that the extruded blend material can be processed under different conditions without changing the co-continuous structure type and without exhibiting significant coarsening.

The correlation between phase structure and blend properties essentially requires the quantification of the co-continuous structure. Some attempts to quantify the co-continuous morphology, primarly based on image analysis of two-dimensional photomicrographs, have been reported;[62] however, investigating a three-dimensional structure by the analysis of a two-dimensional micrograph has obvious limitation: co-continuous structures are complicated 3D interpenetrating and intertwining structures. In spite of state-of-the-art developments in instrumental techniques, morphology determination of polymer blends remains a formidable challenge.[63,64,65] Indeed, methods like light microscopy (LM), scanning electron microscopy (SEM), transmission electron microscopy (TEM) and atomic force microscopy (AFM) may be used to resolve the polymer blend morphology from the millimeter to the sub-nanometer scale,[66] but they image only the surface of the materials and rarely provide information on the internal (bulk) structure.[67] After the seminal work of Verhoogt et al.[68] in

the use of reflection mode laser scanning confocal microscopy (LSCM) to visualize polymer blends, several studies have been reported in literature. In particular Jinnai and co-workers have extensively utilized LSCM to visualize co-continuous structures generated during the late stage of spinodal decomposition of binary mixtures.[69] More recently has been reported that a covalent-labeling of one of the polymer components with a fluorescent dye may enable the possibility to characterize the internal microscopic structure of phase separated polymer blends through laser scanning confocal fluorescence microscopy (LSCFM).[70,71,72] Another useful way to measure the structure shape and the coarseness level (i.e. the phase separation length scale) seems to be the measure of the interfacial area between the phases. Many methods using adsorption technique were reported in the literature, for example by Favis et al.[73]. In this thesis work both approaches were followed: on one side, LSCFM have been used to directly visualize the 3D bulky morphology; on the other side, one method using the time domain nuclear magnetic resonance technique has been put on to evaluate quantitatively and qualitatively the interfacial interactions in a binary chlorinated polyethylene / Nylon terpolyamide blend.

1.6.4 Chlorinated polyethylene/Nylon blends

In section 1.6.2, authors Coran and Patel have been cited as responsible of a wide research studies on rubber/plastic blends. In 1983, they published a paper presenting particular results of blends between chlorinated polyethylene rubber and Nylon.[17] These results were the main source of inspiration for this thesis work.

1.6.4.1 Introduction to chlorinated polyethylene

Chlorinated polyethylene (CPE) is an elastomer produced by random chlorination of polyethylene. It has excellent flexibility and intrinsic chemical, weathering, and ignition resistance, due to the saturated molecular backbone; and it is often cross-blended with thermoplastics and elastomers to improve their properties.[74,75,76,77]

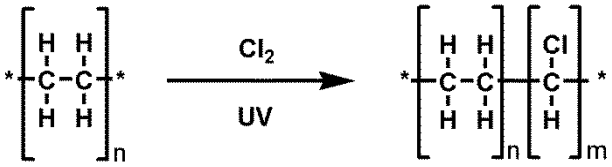

The physical and mechanical properties of CPE highly depend on degree of chlorination, microstructure of polymer chains, method of production and characteristic of the starting high density polyethylene. The rate of the chlorination strongly depends on the distribution and content of substituted chlorine atoms along the CPE's chains. As more and more chlorine atoms are substituted on the polyethylene chain, the crystalline fraction of it gradually reduces and so convert to a softer and more flexible product.[78] The inclusion of the chlorine as a defect in the crystal, while folding and packing chain segments, renders strains in the lattice to a level such that the orthorhombic unit cell of the linear polyethylene crystal is not stable in these systems.[79,80] At low chlorine content the CPE product is still hard. Above the 10% of chlorination the elasticity and flexibility of the product begin to increase progressively and at 35-40% chlorination the reaction product becomes the elastomer. Above 55% of chlorination, the hardness and the toughness of chlorinated polyethylene again starts to increase.[78]

There are two main types of chlorination processes namely: the solution phase and the suspension phase. In the method of solution phase the chlorine atoms are substituted along the backbone of the polymer randomly and homogeneously,

and the obtained CPE has amorphous structure. Most of industrial units produce various kind of CPEs in the solution phase using a single solvent such as CCl_4 or a mixture of solvents.[81] On the contrary, chlorination reaction in the suspension phase (sometimes referred as "slurry phase") mostly happens on the surface of the polymer particles and so the structure of the produced product is blocky and non-uniform. Both of these methods are usually carried out under a moderate pressure. Radical chlorination of polyethylene films in the heterogeneous solid-gas phase is another method of reaction that has been studied more recently,[82] the polymer films that are chemically modified in this way have already found some interesting applications such as membrane technology.[78]

In general, one of the main applications of CPE is as a compatibilizer. In many works present in the literature[83,84,85] CPE is introduced into various polymers and copolymers to improve a number of valuable properties such as oil resistance, flame retardancy, impact strength, etc. One of the most prospective application of CPE is associated with the improvement of the impact strength and processability of poly(vinylchloride) (PVC) used as a major component in different compositions.[83] The efficiency of CPE as impact resistant modifier again depends on its molecular mass, the chlorine content and its distribution along the polymer chains, and of course the amount of CPE with respect to PVC.

Major markets for chlorinated polyethylene elastomers includes various high-performance industrial applications such as hydraulic hoses, wires and cable jacketing for power, ignition wire jacketing and many other industrial parts.

Chlorinated polyethylene has been chosen as the main character of this study, that is, as the soft portion of the prepared thermoplastic elastomers materials, for its versatility and useful properties that may lead to possible applications.

1.6.4.2 Introduction to Nylon terpolyamide

Polyamides are a class of polymers of enduring interest because of their variety, their complex internal structures, their commercial importance and versatility, and their various chemistries of preparation and of long-term use.[86] Until now, most research into polyamide (PA)/rubber blends has been directed towards improving the impact properties of PA.[84] In the present thesis work, instead, the aim is to create a new material with final properties deriving from the synergistic effect of the main rubbery phase and a particular polyamide.

The polyamide used for this work is a random terpolymer between Nylon -6, Nylon -6,6, and Nylon -12. It is a thermoplastic polyamide that combines the inherent toughness of Nylon with ease of processing in solvents as well as melt systems.

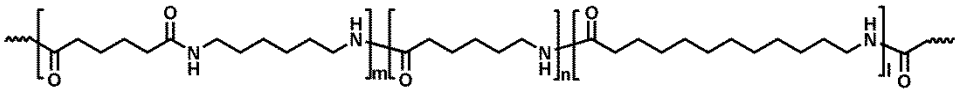

This particular polymer differs from conventional nylons in that it offers alcohol solubility, lower melting (and thou processing) temperatures, and high elongation. Its relatively low melting point (T_m=117 °C) allows the preparation of polymer blends with other systems at lower temperatures where degradation is negligible, and also the curing process in case of TPVs can be performed at lower (cheaper) temperatures.[87] This terpolyamide is suitable to be processed with molding and extrusion; it is though, it withstands impact and resists abrasion, but it is softer and more flexible than conventional Nylons. Concerning the chemical properties, Nylon terpolyamide -6, (-6,6), -12 is insoluble in water, and it resists hot or cold aqueous alkali solutions and most salt solutions for weeks or months. Acetic acid attacks the material slowly; stronger acids react more rapidly; formic acid will dissolve it very effectively. Most oxidizing agent react with Nylon terpolyamide -6, (-6,6), -12 but oxygen and oxygen-containing gases like ozone have little effect. It is also highly resistant to petroleum based products, showing

little change after prolonged contact with lubricating oils and greases, or aliphatic and aromatic hydrocarbons.[88] This is really outstanding, in particular concerning the benefits for applications in the field of thermoplastic elastomers from rubber/thermoplastic binary blends.

For all these reasons, Nylon terpolyamide -6, (-6,6), -12 has been the candidate as the hard thermoplastic portion in the materials presented and studied in this thesis work.

1.6.4.3 Chlorinated polyethylene/Nylon blends

In the work from Coran and Patel, both non-cross-linked and dynamically-cross-linked thermoplastic/rubber compositions from various Nylons and chlorinated polyethylene where prepared in a Brabender Plasticorder at 225 °C. A cold milling process after internal mixing ensured uniform dispersion of discrete Nylon particles in the rubber matrix. One point gained the attention of the authors and inspired the work that is going to be presented in this thesis work: the mechanical properties of the prepared blends, and especially the tensile strength, were much higher than expected. The author could not be able, with the techniques available in the 1980s, to resolve the microstructure of the blends, neither to deeply investigate the interfacial interactions between the two phases. Consequently they were not able to give explanation of the macroscopic behavior from the structure-properties relationships standpoint. They only found that a chemical interaction between CPE and Nylon resulting in graft formation within the polymer chains was responsible for the high mechanical strength of the compositions. They proved this conclusion in a rather speculative way. After selective extraction of the hard phase with formic acid (that is not affecting the CPE anyway, but is very effective for dissolving the polyamide), infrared spectra of the extracted compositions gave traces of the absorption maxima associated to the Nylon's amide group.

The following two mechanisms were suggested by the authors for the graft formation:[17]

1. Aminolysis of halogenated polymer by a terminal amine group of Nylon:

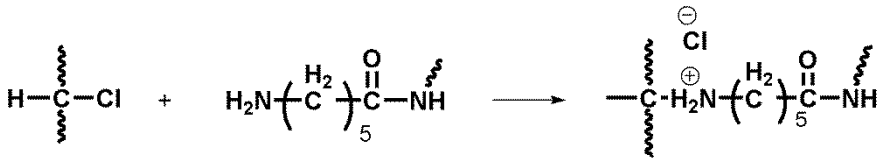

2. Alkylation of the Nylon amide group by chlorinated site of the CPE chain:

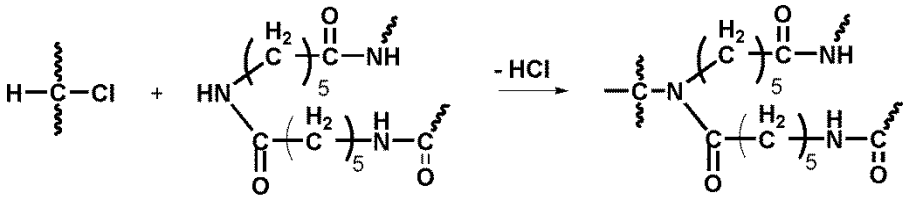

It is expected that the graft copolymer can reduce the interfacial tension between the two phases and promote adhesion between them.

The superior mechanical properties of the cross-linked systems are due to the stabilization of the rubber particulate morphology which resulted from cross-linking. This could prevent reagglomeration and coalescence of the rubber particles after the mixing process. In general, the smaller the particle size of the dispersed rubber phase are, the better will be the mechanical properties of the system.

However, the authors, as said before, were not able to directly see the phase separation of the thermoplastic elastomers obtained. Furthermore, the interfacial interactions discovered, even if confirmed by Liu et Al.[84], were not properly detected. The ultimate properties of the compositions were calculated as function of the surface energy mismatch between the polymers, crystallinity of the hard phase, and the critical chain length for the rubber molecule entanglement, as purposed by the authors themselves.[13] The best compositions were those in which

the surface energy mismatch between polymer was a minimum. The Young's moduli of the non-vulcanized compositions, for example, were calculated from the following equation:

$$E = \phi^{n}_{H}(n\phi_S+1)(E_U-E_L) + E_L$$

where F_H is the volume fraction of the hard phase, F_S is the volume fraction of the soft phase, and E_U and E_L are upper and lower bound Young's moduli respectively:

$$E_U = \phi_H E_H+\phi_S E_S$$

$$E_L = (\phi_H/E_H+\phi_S/E_S)^{-1}$$

The value of *n* is related to the change in phase morphology as a function of the concentration of the hard phase.

The morphology of the phases within the bulk of the material and the interfacial interactions between them are, in fact, the most important parameters to evaluate in order to explain the structure properties relationships.

As described in the previous section, a co-continuous morphology would give several advantages for the final properties of a material consequently of the co-continuous phase formation.

In conclusion, very few works are present in the literature. Rudolph et al.[89] obtained the best retention of tensile and flexural modulus and strength characteristics by toughening Nylon with chlorinated polyethylene, but they concluded their paper saying that any further understanding would require more extensively basic study. This open the research path aimed to understand the structure properties relationships in these CPE/Nylon thermoplastic elastomers.

1.6.5 Processing methods for TPE blends

As described before, one of the biggest advantage in having a thermoplastic elastomer is the possibility to use easy processing suitable to thermoplastic in order to obtain the final material. There are several processing methods widely used to process TPEs from rubber/plastic binary blends, the most important are the mixing and the injection molding; these two processes will be briefly discussed here as they were used to obtain the samples presented in this thesis work.

Blends of rubber and thermoplastic are mostly prepared by melt-mixing the polymers in a internal mixer. The parameters that have to be set are rotor speed; residence time; and temperature. The temperature of mixing must be above the melting point of the plastic, and the rotor speed, after the melting, must increase. The longer the mixing time is, the better the dispersion of the components in the blends, in the thermoplastic, state would be. Anyway, in order to avoid decomposition, mixing times usually should not be over ten minutes. During the mixing process, the torque initially increases, because of the decrease in temperature of the preheated chamber on incorporation of the plastic. As soon as the plastic starts melting, there is a decrease in torque which again increases on addition of rubber; after the rubber attains the temperature, the torque again decreases. The blends obtained from the internal mixer are further plasticized and sheeted out under hot conditions through the open mill set at few millimeters nip gap.[7]

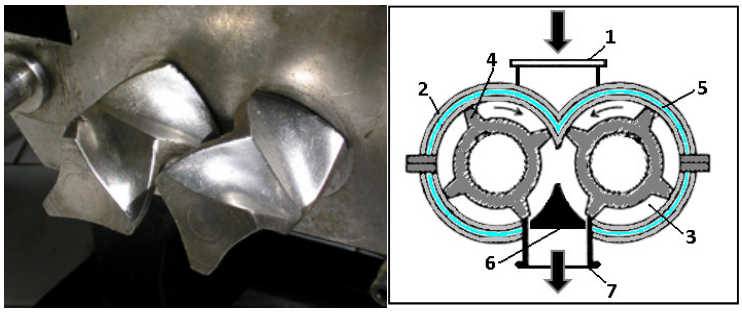

Figure 1.8: Picture of the two-wing rotors of the internal mixer (left). On the right: schematic drawing of a Brabender internal mixer; 1-feed hopper, 2-chamber walls, 3-mixing chamber, 4-rotors, 5-cooling system, 6-saddle, 7-discharge slide.

After the preparation of the blend, injection molding is the most widely used industrial process for fabricating thermoplastic elastomers parts.[2,5] It fully exploits the processing advantages of thermoplastics. Elimination of scrap and shorter cycles of this molding outweighs the higher material cost of TPE compared to a thermoset. Injection pressure and rate, plus mold temperature and cycle time are the most important parameters to set in order to achieve the final product. The operating temperature for processing normally lies in the range of 20 – 50 °C above the melting point of the hard portion to allow adequate mold packing and minimum shrinkage.

1.6.6 Applications, growth and future

Over the last 10 years, all the families of thermoplastic elastomers have gained widespread recognition as an ideal material for a broad range of applications. The principal success of TPEs have derived from their replacement of thermosets rubbers, either directly in the existing application or in new applications that otherwise would have specified thermosets compounds. The fact that TPEs do not require vulcanization is of course the key point of this growth.

TPEs also offer several environmental benefits, for example scraps generated during production maybe usually reground and recycled.[2]

Present market and applications of TPEs from hard polymer/elastomer blends is still dominated by the automotive. The excellent weatherability of these materials, their low density and relatively low cost make them a common component in a number of exterior and interior automotive applications. Another large market of thermoplastic elastomers blends is wire and cables.[7] Excellent electrical properties, in combination with ozone and water resistance make these materials an ideal choice for a number of low voltage and cable applications. In those applications that require flame resistance or low smoke generation, many of the same compounding ingredients used to manufacture flame retardant cured rubber and plastics have been successfully used to produce competitive rubber / plastic formulations. Finally, miscellaneous molded and extruded goods represent another huge market of such materials, especially for applications in grips.[90]

Figure 1.9: Some typical present application for thermoplastic elastomers from non-vulcanized binary rubber/plastic blends (grips, sports goods…). Images taken from the WWW.

Since 1970s, TPEs in general have enjoined a compounded annual growth rate of 8%-9% in the market, in contrast to the low growth rate of rubbers (1%-2%) and plastics (3%-6%) industries. In particular, in the European market area, thermoplastic elastomers from non vulcanized rubber/plastic combination

occupied, in the last decade, the second place in the overall consumption, after styrenic block copolymers.[7] As introduced before, growth of TPE usage is due to three main factors: replacement of other materials, new processing technologies, and new applications and markets. TPEs have proven themselves in meeting a wide range of demanding engineering requirements and automotive applications. These applications will continue to grow because of the cost savings provided and the performance delivered. TPEs will continue to replace thermoset rubbers for applications in which they offer cost advantages and design flexibility to the automotive engineer. World demand of thermoplastic elastomers has grown more than 6% per year even in 2009.[91]

For all these reasons, TPEs have been widely studied both in industrial and academic field. For example, many efforts are spent to overfill one big limitation in the TPEs application: the largest end use of conventional rubbers, that is, automobile and truck tires. With the help of the recent discoveries in nanotechnologies and nanostructured materials, many research groups are developing new rubber/plastic blends filled with nanowires, carbon nanotubes and so forth.[92] Another important example of a new research field of TPEs blends is the developing of biodegradable TPEs,[93] this is mainly due to the recent changes in environmental regulations, that are forcing manufacturers to become more responsible for the safe disposal and the recycling. TPEs are gaining and will capture more ground also in the medical supply and artificial organs market, as replacement materials for thermosets with all the performance advantages and low processing costs. Artificial implants and soft tissue replacement are effective research fields for TPE from rubber/plastic blends, nowadays.[2]

2 Chapter Two: Materials and Processes

The polymers used for the compositions have been presented in depth in the previous chapter and their particular properties have been discussed. For the obtaining of the samples, the classic methods for mixing and processing thermoplastic elastomers, also described before, were used.

In this chapter, some preliminary characterization of the chlorinated polyethylene rubber main phase will be given; and after that, all the processes used for the preparation of the materials will be described in details.

2.1 Starting materials

The polymers used in the present work are chlorinated polyethylene rubber Tyrin™ CM 3630E Chlorinated Polyethylene Resin from Dow® Polymer with 36% of chlorine weight content (medium viscosity grade with low crystallinity, obtained with slurry state chlorination process); and co-polyamide Elvamide® 8066 Nylon Multipolymer Resin from DuPont®, a terpolymer of Nylon 6, (6-6) and 12 with a melting point of 117° C.

Some preliminary characterization on the chlorinated polyethylene has been performed in order to check the chlorine distribution along the polymer backbone and the degree of polymerization of the constituting high density polyethylene. Further analysis has been done to control the different polarity of the chosen rubber and thermoplastic phases.

^{13}C-NMR (Nuclear Magnetic Resonance) spectroscopy was performed on a AMX 500 Bruker Spectrometer after complete dissolution of the polymer under reflux conditions with benzene-d_6 as the solvent. A recycle delay of 4 seconds provides quantitative relations between the integrals of the peaks; and 5.000 scans in the experiments gave quite satisfactory signal to noise ratio.

The spectrum for chlorinated polyethylene is depicted in Figure 2.1, the peaks were compared with those reported in the literature for poly (vinyl chloride) and chlorinated polyethylenes.[94]

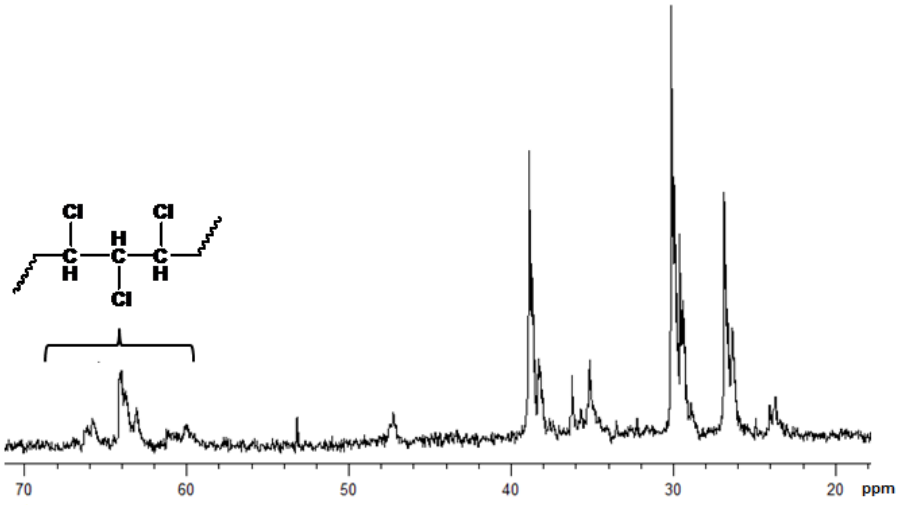

Figure 2.1: solution ^{13}C – NMR of Chlorinated Polyethylene (CPE) in deuterated benzene.

At first glance, is it quite clear that along the polymer chain the most common situation is to find –CHCl–CHCl–CHCl groups more than isolated –CHCl– sites. None $–CCl_2–$ unity are present along the chains.[95] In conclusion, the "blocky-like" structure of a chlorinated polyethylene obtained by slurry-state chlorination process is confirmed by the clusterization of the chlorine atoms in the polymer main chain.

Gel permeation chromatography (GPC) was conducted using THF (Cromasolv grade) as the eluent (flow rate 2 mL/min, 30° C) with a Waters 1515 HPLC Isocratic Pump and a Waters 2414 Refractive Index Detector. Toluene was used as the internal standard. Polystyrene standards were employed for the SEC calibration.

Figure 2.2 depicts the gel permeation chromatograms for the chlorinated polyethylene.

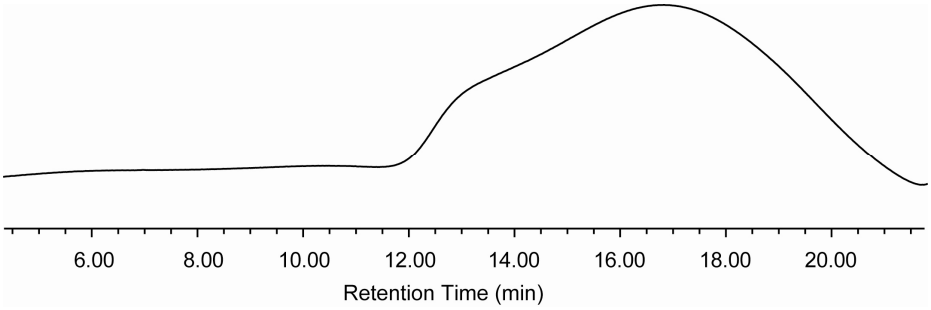

Figure 2.2: Gel permeation chromatogram in THF of Chlorinated Polyethylene (CPE).

By the extrapolation of the data from the gel permeation chromatography analysis, is it possible to calculate the polydispersity index *D*, with the formula

$$D = M_w/M_n$$

were M_w is the weight average molecular weight, and M_n is the number average molecular weight. It indicates the distribution of individual molecular masses in a batch of polymers. For the examined chlorinated polyethylene, the polidispersity index is then:

$$D = M_w/M_n = 278.083/64.164 = 4.33.$$

This is a quite high value for a normal polymer, probably due to the effect of the random chlorination process suffered from CPE.

Water Contact Angle measurements were performed with a PGX pocket goniometer (FIBRO systems) using 2 µL droplets, with 5 or 6 repetitions for each sample. Samples of pure chlorinated polyethylene and Nylon terpolyamide were prepared by injection molding as described in the next section and flat regions of the specimens were chosen for the deposition of the drop.

The surface energy is an important parameter that characterizes the interfacial behavior of a material. The different wettability between elastomers and plastics,

called surface energy mismatch, can give an estimation of interfacial tension between them during melt mixing and can affect the morphology of the final material; in particular, the size of the dispersed particle of one phase, or the phase separation length scale, in case of co-continuous morphology.

In Figure 2.3 the results of contact angle experiments are presented.

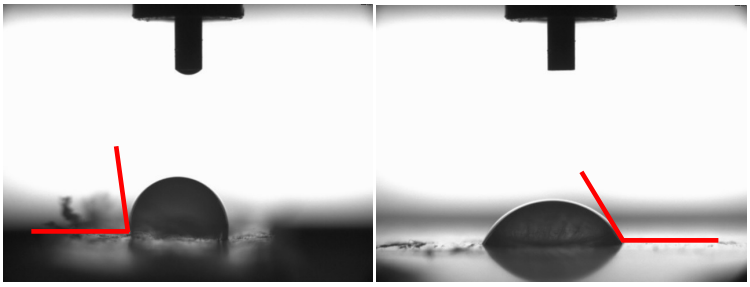

Figure 2.3: contact angles of a water drop on chlorinated polyethylene (left) and Nylon terpolyamide (right) surfaces.

The angles with which the water wet the surface of the two materials are very different. In the first case (CPE) the angle formed with the surface is less than 90°, that means that the material's surface is lipophilic. The surface of the PA, on the contrary, seems to be rather polar, i.e. hydrophilic, as the water makes an obtuse angle with its surface.

These results suggest that the surface energy mismatch between the two materials should be substantial. In the next chapter, it will be demonstrated that, despite this energy mismatch, specific interaction between the polymers chains at the interface cause compatibility in the blends, with consequently enhanced final mechanical properties.

2.2 Internal Mixing

Nylon copolymer (PA -6, -(6,6), -12) pellets were dried in vacuum oven at 80°C for 4h before blending. The blends were compounded in a Haake Rhecord internal mixer fitted with Banbury type rotors and having 200 ml volume chamber, preheated to 150° C before putting in the materials. Five blends were prepared with CPE:PA ratios of 90:10, 80:20, 70:30, 60:40, 50:50 by weight. MgO was added with the two polymers in the amount of 2 phr referred to the rubber content. Blending was allowed to proceed for 420 seconds at a temperature of 180° C and 80 rpm rotor speed. After that the materials were plasticized for few minutes in an open-mills mixer obtaining sheets of 3 mm thickness. Despite the starting materials were colorless or whitish, the final mixtures appeared transparent but light-brown/orange colored.

2.3 Injection Molding

The materials were then cut in little pieces and injection molded in a Ray Ran Injection Molding Machine under the pressure of 0.7 MPa in a mold of shape and dimensions shown in the picture below.

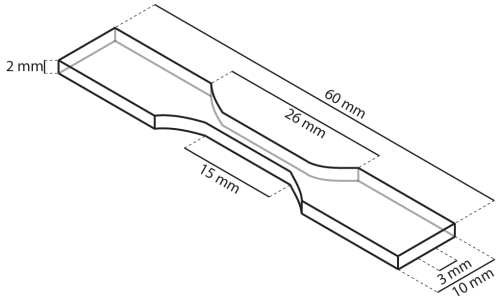

Also specimens of pure CPE and pure PA were prepared and the temperatures set for the barrel and the tool (mold) are reported in Table 2.1.

Table 2.1: molding temperatures for the preparation of the CPE/PA blends' samples.

	CPE	90:10	80:20	70:30	60:40	50:50	PA
Barrel T (° C)	150	160	155	150	140	130	125
Tool T (° C)	120	130	130	130	120	120	80

Samples have been taken under pressure for 60 seconds and then cooled down slowly at room temperature for 300 seconds. Besides Polyamide, blends with more than 20 wt.% of thermoplastic content presented a good dimensional stability during injection molding. It has to be noted that obtaining injection molded samples without significative shrinkage is already a result, as it means that the samples are able to be processed as thermoplastic materials.

In the graphic in Figure 2.4 the different densities of the various obtained blends are plotted versus the Nylon terpolyamide content.

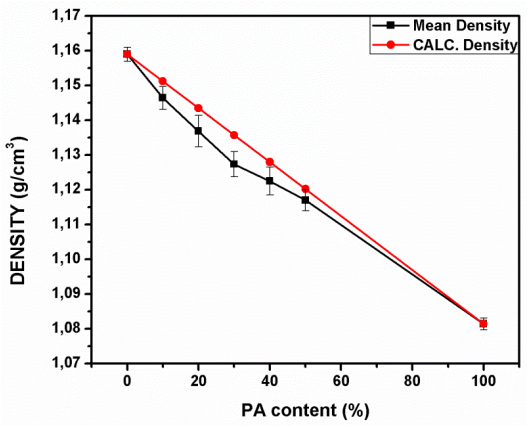

Figure 2.4: Densities (in g/cm^3) of the CPE/PA blends. Red line represent the calculated density as a weighted average of the pure components at that ratio.

Thermoplastic elastomeric blends are normally less dense in respect to the starting materials.[5] This decrease in density is sometimes due to the arrangement of the phases (in case of phase separated systems) and in particular to a finer and more effective dispersion or mixing.

By looking at the graphic, thou, and specifically at the fact that the density is decreasing fo the blends respect to the pure components' weighted average, is it possible to dare the speculative assumption that the components are some kind compatible, and in 60:40 CPE/PA (w/w) composition the finest dispersion is reached.

Next chapter will give confirmation of this assumption from the standpoint of the macroscopic mechanical behavior; chapter four will grant further corroboration at the fact that the two phases are compatible at the interface; and, finally, chapter five will award this initial hypothesis proving the microstructure of the samples by direct visualization of the three-dimensional bulk of the materials.

3 Chapter Three: Macroscopic Behavior

Checking the macroscopic mechanical properties is the very first step for knowing immediately the thermoplastic elastomeric behavior of the materials in exam. Tensile tests and dynamical mechanical investigations are the most commonly used and straightforward way to characterize the mechanical properties of polymer blends.

3.1 Mechanical properties

3.1.1 Experimental

Tensile tests were performed directly on the specimens as prepared with injection molding using a mechanical testing machine Zwick 1445 with a load cell of 500N. Experiments were carried out at room temperature with a test speed of 200 mm/min. Tensile strength, elongation at break and elastic modulus have been determined as averages of three independent drawing experiments performed at the same conditions. The elastic modulus was calculated as the slope of the straight fitting the curve between elongations of 0.02 to 0.04 $\Delta l/l_0$.

3.1.2 Tensile tests

The fundamental transitions between rubber, thermoplastic and plastic behavior as a function of the CPE/PA ratio are clearly reflected in the mechanical properties of the blends, which were characterized by tensile tests. Typical stress-strain curves of the pristine polymers and blends with CPE/PA ratios from 90:10 to 50:50 by weight are presented in Figure 3.1 a. For pure CPE and for the blends with 90:10 and 80:20 (w/w) CPE/PA ratio the materials show rather low moduli and considerable elongations, typical behavior for unvulcanized or undervulcanized rubber. Conversely, curves for pure PA and 50:50 (w/w) CPE/PA composition present a narrow yield point and a consistent plastic deformation plateau typical for thermoplastic polymers. Finally, relevant mechanical properties are found with compositions CPE/PA of 60:40 and 70:30 by weight. In this case, the shape of the curves is that typical of thermoplastic elastomers, and the curves do not present any plastic deformation before failure (Figure 3.1 a).

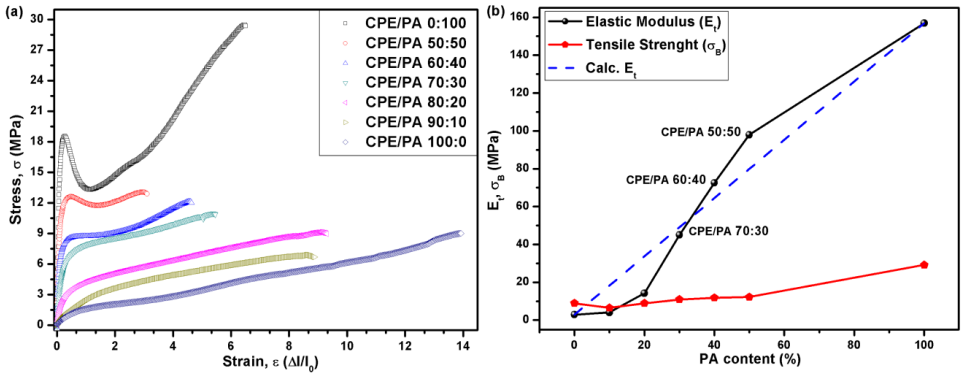

Figure 3.1: (a) Stress-strain curves for CPE/PA blends. (b) Elastic modulus (E_t) and tensile strength (σ_B) as a function of CPE/PA ratio in the blends. Dashed line represents weight average of the E_t of pure components.

The elastomeric behavior of a polymeric material is commonly quantified through its elastic modulus (E_t), that can be easily extracted from the initial slope of stress-strain curves like those depicted in Figure 3.1. The elastic moduli of the CPE/PA 60:40 and 50:50 (w/w) blends show higher values than the simple linear combinations of the two components (Figure 3.1b). Moreover, Figure 3.1b shows that the components are compatible since the elastic moduli increase with the increase of PA content, while tensile strength stays rather constant.

Stress-strain behavior typically depends strongly on the properties of the matrix component, making phase inversion, in a phase separated polymer blend, easily detectable. In co-continuous blend compositions, both phases fully contribute to the blend modulus in all directions as a result of the effective stress transfer.[33] Therefore the moduli are very high and appear to be isotropic. In addition, synergistic effects can rise affecting the tensile properties of the final material.

Table 3.1: Mechanical properties of the CPE/PA blends. In the last column are presented the values predicted from a weighted average between the values of elastic moduli of the two pure components.

	σ_B (MPa)	ε_B (%)	E_t (MPa)	Calc. E_t (MPa)
PA	**29.4**	**650**	**157**	
CPE/PA 50:50	**12.9**	**309**	**98**	**80**
CPE/PA 60:40	**12.0**	**463**	**72.5**	**64.5**
CPE/PA 70:30	**10.9**	**545**	**45**	**49**
CPE/PA 80:20	**9.0**	**929**	**14**	**33.5**
CPE/PA 90:10	**6.8**	**887**	**4**	**18**
CPE	**9.0**	**1378**	**3**	

3.2 Rheology

3.2.1 Experimental

Dynamical Mechanical Analysis (DMA) was performed on a Rheometrics RMS 800 mechanical spectrometer. Shear deformation was applied under conditions of controlled deformation amplitude, which was kept in the range of the linear viscoelastic response of studied samples. Plate-plate geometry was used with plate diameters of 6 mm. Specimens were cylinders of 6 mm diameter and about 2 mm thickness manual die cut from the samples obtained by injection molding. Experiments have been performed with a 2 °C/min heating rate under a

dry nitrogen atmosphere. Results are presented as temperature dependencies of the storage (G') and loss (G'') shear moduli measured at a constant deformation frequency of 10 rad/s.

3.2.2 Building of the mastercurve

The first experiment was the obtaining of a master curve with the time temperature superposition on the sample that revealed the most interesting mechanical tensile behavior, i.e. CPE/PA 60:40 (w/w) blend.

The specimen for the DMA was obtained by manual die cutting the dog-bone-shaped specimen as obtained by molding, choosing a zone where the sample was rather flat. The specimen's shape was a cylinder with 6 mm diameter and 2.36 mm thick. The geometry used for the experiments was, therefore, the parallel plates.

Before starting the machine was equipped with the liquid nitrogen, in order to have a temperature range widely below the room temperature.

Than, good contact between the two parallel plates and the faces of the specimen was needed, so the temperature was increased to 80° C in order to soften the material and a little vertical strength was applied, then released and set to a little value, enough to maintain a good contact.

As first thing a Dynamic Strain Sweep (DSS) experiment was performed with temperature set to T = 80° C and the frequency set to $\omega = 10$ rad/s, varying the strain from $\varepsilon = 0.1\%$ to $\varepsilon = 10\%$ and measuring the torque. Once obtained the curve, the torque has been set, in the next experiment, to $\varepsilon = 0.5\%$, in order to stay in the linear behavior zone of the stress-strain curve.

The next experiment was a Dynamic Frequency Sweep (DFS), with T = 80° C, ε = 0.5% and varying the frequency from ω = 0.1 rad/s to ω = 100 rad/s. A graphic where G', G", η and Tanδ were plotted versus ω was obtained.

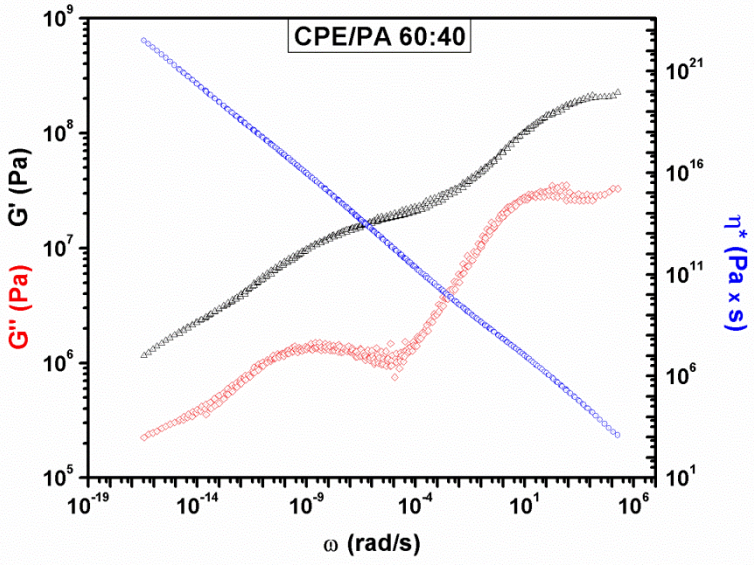

Figure 3.2: Storage modulus (G'), loss modulus (G"), and complex viscosity plotted in logarithmic scale against the oscillation frequency for the CPE/PA 60:40 (w/w) blend.

The master curve has been built up choosing as reference curve the one taken at -15° C, because this temperature is very close to the lowest glass transition temperature of the sample.

The graphs of the master curve and of the time-temperature superposition shift factors are reported below in Figure 3.3.

The master curve built up for this sample does not give too much information, because the red curve of the loss modulus G" never crosses over the black curve

of the storage modulus G' (see Figure 3.2); so it is not possible to know the maximum energy absorption and damping in the time scale; and is also possible to say that, in this range of temperature (T: +80° ÷ -24° C), the material does not flow.

Furthermore, by looking at the G" curve, it is possible to see that at the frequency of $\omega = 10$ rad/sec a segmental relaxation of the polymer chains occurs.

The viscosity decreases linearly with the frequency, as expected.

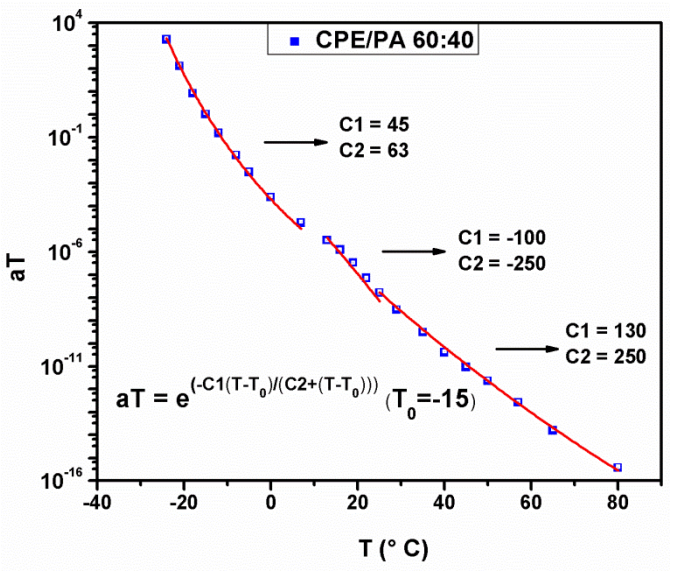

Figure 3.3: Time Temperature Superposition Shift Factors Vs. Temperature for the CPE/PA 60:40 (w/w) blend and its interpolation (in red) with the William-Landel-Ferry equation.

From Figure 3.3 it is clear that the curve of the shift factors can not be fitted by one only WLF equation: it is possible to see two different behavior due to two different processes, one dominating at lower temperatures and one dominating at

highest temperatures. In the region from T = 5° C to T = 20° C the material is below the first glass transition temperature: extrapolation to temperatures below T_g might be considered erroneous.[96] When the constants are obtained with data at temperatures below T_g, negative values of C_1, C_2 are obtained, which are not applicable above T_g and do not represent Arrhenius behavior.

In conclusion, these facts might be a first confirmation that we are at the presence of a two phase-separated system.

3.2.3 Dynamic ramp temperature test

Figure 3.4 depicts results presented as temperature dependencies of the storage (*G′*) and loss (*G″*) shear moduli measured at a constant deformation frequency of 10 rad/s for all the CPE/PA blends.

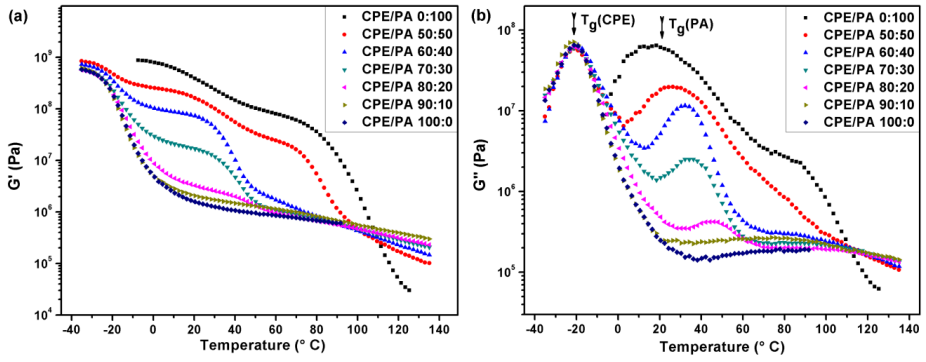

Figure 3.4. (a) Storage modulus (G') and (b) loss modulus (G") from DMA measurements as a function of the temperature for the reported blends.

The corresponding room temperature values of the storage modulus G', measured by dynamic mechanical analysis, confirms the trend of the Young moduli as calculated from the stress-strain curves in previous section. The DMA curves in Figure 3.4a were obtained on cooling, after the samples were initially

heated slightly above the melting temperature of the PA. At room temperature the polyamide is the stiffest material with G' = 320 MPa. This high value decrease only slightly to ~140 MPa and ~70 MPa for blends with CPE/PA ratios of 50:50 and 60:40 (w/w) respectively. On other hand pure CPE and blends with 90:10 and 80:20 (w/w) CPE/PA compositions are significantly softer materials, with G' values of around 1-3 MPa. The blend with a 30% of PA features an intermediate behavior.

The nonlinear dependence of the elastic properties on the composition is strongly related to the blends morphology. The behavior of loss modulus curves (Figure 3.4b), clearly shows that basically at all CPE/PA ratios the two polymers in the blends are phase separated, since two different glass transition temperatures are present.[97] The dynamic mechanical analysis, however, do not provide any information neither on the type of phase-separated morphology nor on its characteristic length scale.

4 Chapter Four: Interfacial Interactions

Interfacial interactions and interphases play a key role in all multicomponent materials. Recognition of the role of the main factors influencing interfacial adhesion and proper surface modification may lead to significant progress in many fields of research. In polymer blends, the interactions between the components at the interphase are a dominating factor. Interaction or the lack of it determines miscibility, phase structure and properties of the blends.

This chapter, with the aid of various traditional or more sophisticated techniques, aims to describe the interfacial effects detectable in chlorinated polyethylene / Nylon terpolyamide blends, and to describe how the analysis of these interactions can affect the structure and, accordingly, the macroscopic properties of the final material.

4.1 Absorption maxima in IR bands

Though polymeric blends that gives thermoplastic elastomers are, by definition, immiscible, they have to display favorable intermolecular interactions to obtain the necessary interfacial adhesion allowing the desirable improvement in properties. In many cases, the origin of the intermolecular forces causing compatibility is not wholly known, therefore the application of techniques leading to the detection of characteristic features of these phenomena is particularly interesting. One of the techniques used in this kind of study is the Fourier Transformed Infrared Spectroscopy (FT-IR). The position, form and intensity of spectral bands provides useful information about the microstructure of polymers at a molecular level, although, in most cases, the effects of intermolecular forces on the spectrum are small, due to its low energetic level as compared to the interchain covalent bonds.[98] In any case, FTIR spectroscopy has been widely used to study miscibility/immiscibility of polymer blends, especially when relatively strong interactions are revealed, as, for example, hydrogen bonds.[99,100]

4.1.1 Experimental

Attenuated total reflection Fourier transform infrared spectroscopy (ATR-FTIR) spectra of the injection molded specimens were recorded using a Spectrum 100 FT-IR Spectrometer (Perkin Elmer, USA) in the range of 4000-650 cm^{-1}. The spectra were obtained after 256 scans at 2 cm^{-1} resolution.

4.1.2 Comparison of the absorption maxima

In Figure 4.1 the region corresponding to the N-H stretching mode of the amide groups (left) and the C-Cl stretching mode of chlorinated polyethylene (right) are depicted.

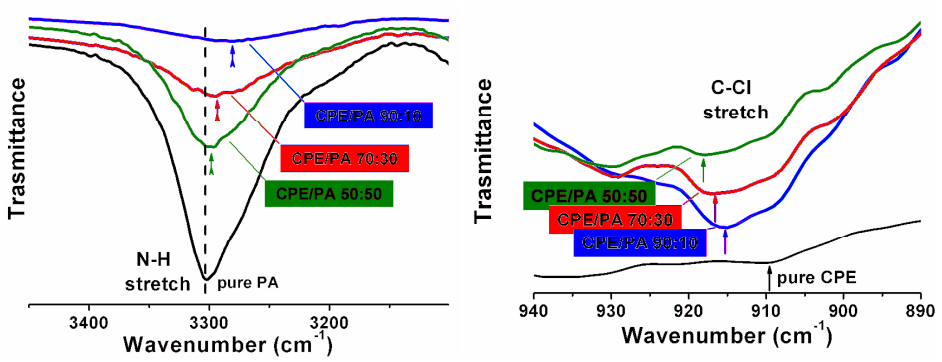

Figure 4.1: infrared spectra in the region of 3200 – 3400 cm^{-1} (left) and in the region of 900 – 940 cm^{-1} (right) for CPE/PA 90:10, 70:30 and 50:50 (w/w) blends.

At first sight, displacements can be observed in the absorption maxima of the bands, compared to pure PA and pure CPE spectra. This means that some of the dipoles existing in the polymers undergo vibrational alterations due to the change in their environment caused by the presence of another component. Alteration occurs by the participation in intermolecular interaction which make the partial miscibility possible; so such changes should account for partial miscibility at the interface between the soft chlorinated polyethylene phase and the hard Nylon terpolyamide phase.

With this characterization is it possible to discern such interaction, but none information is provided about the type of interaction. In particular, it is not possible to say if the interfacial miscibility occurs, at room temperature, between the amorphous phases of the components, or around the crystallites of the crystalline phase of the hard portion. The following characterization techniques, presented in this chapter, (Time Domain Proton Nuclear Magnetic Resonance and Differential Scanning Calorimetry) are aimed to investigate about this topic.

4.2 Relaxation of polymer chains

4.2.1 Introduction to TD-^{1}H-NMR

The theoretical basis of NMR[101] is that when nuclei with nonzero spin *S*, such as ^{1}H, ^{2}H, ^{13}C, ^{19}F, ^{129}Xe and many others, are immersed in a constant magnetic field B_0, their energy levels E_m split according to the values of the magnetic quantum number *m* (which goes from –*S* to *S* in integer steps) as $E_m = \gamma\hbar m B_0$, where γ is the gyromagnetic ratio of the nucleus. The Boltzmann law of statistical mechanics gives the equilibrium population of these energy levels as a function of the sample temperature *T*. As low energy levels are more populated, a macroscopic magnetic moment *M* develops parallel to B_0:

$$M = \frac{N\gamma^2\hbar^2 S(S+1)}{3kT} H_0 = \chi_0 B_0,$$

where *N* is the number of nuclei in the sample. This is known as Courie law.

Transitions between different energy levels are possible through the absorption and emission of electromagnetic radiation. In NMR experiments a sample immersed in a static magnetic field is irradiated with electromagnetic pulses of appropriate frequencies in order to perturb thermodynamic equilibrium and the recovery of equilibrium (relaxation) of the system is followed experimentally by measuring the emitted radiation.

A theoretical description of this phenomenon can be quite complicated as depending on dynamics of the whole system and not of only spins. Despite this, the following phenomenological approach due to Bloch has proven very useful in reproducing many observations. Basically the idea is to introduce some ad hoc modifications to the equation of free spins in order to account for the relaxation process.

The behavior of a magnetic moment M in a magnetic field B is described by the following equation

$$\frac{dM}{dt} = \gamma M \times B \qquad [1]$$

If $B = B_0$ is a static filed, then this equation tells us that the magnetic moment M is preceding around the direction of B_0 with frequency $\omega_0 = -\gamma B_0$.

Suppose now that electromagnetic radiation is applied to the sample. We may represent it introducing a field B_1 rotating in the plane perpendicular to H_0, with frequency ω: $B = B_0 + B_1$. In this case the dynamics of $M$is better described in a frame rotating with H_1. In this frame the magnetization rotates with frequency $\omega_e = -\gamma B - \omega$. In NMR experiments H_1 is usually much smaller than B and most importantly ω is as close as possible to ω_0. In this way $\omega_e \sim -\gamma B_1$ and the applied pulse to rotates M around a direction perpendicular to B_0. For example suppose that M is in its equilibrium position parallel to B_0. With the application of an NMR pulse appropriate time (p90) we can rotate the total magnetization, into the plane perpendicular to B_0, and by doubling this time (p180) M is rotated of 180°. When the E.M. pulse is switched off, according to equation [1] the magnetic moment M starts preceding around the static field B_0. Hence equation [1] doesn't describe the return to the equilibrium value through relaxation. In order to account for relaxation Bloch proposed to modified equation [1] as follows:

$$\frac{dM}{dt} = \gamma M \times H - R(M - M_0),$$

where M_0 is the equilibrium magnetization, which is supposed to be in the z direction, and

$$R = \begin{pmatrix} 1/T_2 & 0 & 0 \\ 0 & 1/T_2 & 0 \\ 0 & 0 & 1/T_1 \end{pmatrix}.$$

According to this equation the magnetization returns to its equilibrium value in an exponential manner. The component along B_0 with a constant of time T_1 called longitudinal relaxation time, the component perpendicular to H_0 with a different time T_2 called transversal relaxation time.

T_2 measurements where performed on Chlorinated polyethylene / Nylon terpolyamide blends samples. The experimental task of measuring T_2 is further complicated by field inhomogeneity: the spins precess with slightly different frequencies depending to their position in the sample. The result is a dispersion of local magnetic moments in the xy plane with the consequent cancellation of the various contribution. Hence if we simply apply a p90 pulse and measure the decaying of the yx component will be much faster than expected. The solution to this problem was found in the concept of echoes: after a time τ of free evolution the sample a 180° pulse is applied to the sample which reverts the order of spins. After another τ sample all the spins results again aligned ad the magnetization can be measured. By varying τ in successive experiments the evolution can be followed and T_2 is determined. This experiment is called Hahn echo.[102]

Even though not directly linked to the measurement of T_2, the simple measurement of the free behaviour of the magnetization after a p90 pulse (FID) is rich of information. However another technical problem arises: it is technically impossible possible to swith off the E.M. pulse instantaneously. This implies that the first part of the evolution is lost as its measurement would be useless. This is a serious issue in solid samples were the FID decades very rapidly. The MSE approach is a very clever approach to circumvent this problem and allows to measure a larger part of the FID.[103]

In conclusion, while in conventional NMR the signal is Fourier-transformed in order to obtain information on the small shift in the energy levels E_m due to the influence of the nuclear neighbourhood (chemical shift), in TD-NMR relaxation signals are analyzed directly. The information on the chemical environment of each nucleus is neglected, but the analysis provides information on the molecular mobility of different nuclei. In the case of the protons in polymers, this can be related to chain mobility, presence and quantity of rigid and mobile phases and interaction between different chains.

4.2.2 Experimental

A 0.5 T Bruker Minispec was used for this work. This instrument is a low resolution NMR spectrometer with proton Larmor frequency of 19.9 MHz, equipped with a static probe and a BVT3000 heater temperature control unit working with nitrogen gas. Temperature was calibrated using an external thermometer with an accuracy of ±1 K. The precision is 0.1 K and the temperature is stable within that range during the measurement. A typical sample was made of a disk with a diameter of 6 mm manual die cut from the same region. Such disks were positioned into a NMR glass tube with 10 mm external diameter and 8.8 mm internal diameter and the tube was accurately positioned in the NMR cavity in order to guarantee the most homogeneous static magnetic field and radiofrequency pulses.

The samples were left at least ten minutes in the magnet to ensure thermal equilibration before starting the experiments.

For the 90°, pulse length was set to 2.85 μs. Good signal to noise ratio was obtained within few scans, but due to the analytical nature of this work each sample was measured with 128 scans in order to minimize noise.

Figure 4.2 gives an example of a typical FID curve of a solid material, constituted by a hard and a soft part. In this kind of measurements phase resolution is based on T_2 differences between the phases: polymer phases with higher mobility display longer transverse relaxation times. These differences depend on dipolar coupling, so they are field-independent. In this work, we compare results using both the mobile and the rigid phase. The equation presented in Figure 4.2 is the one used for the deconvolution of the FID curve and the calculation of the hard/soft ratio in the material. Relaxation of the rigid part is fitted with a Gaussian function, while the mobile phase is represented by a stretched exponential.[104]

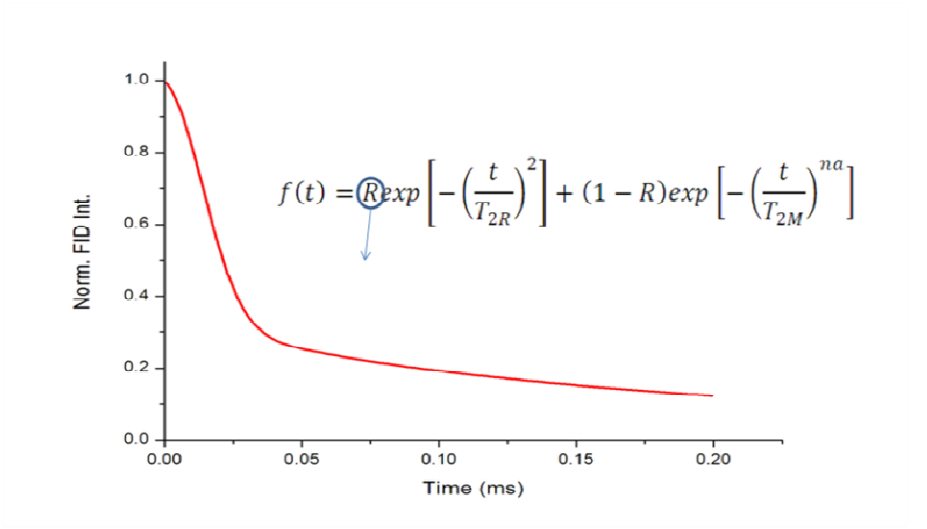

Figure 4.2: Typical FID curve acquired with a MSE refocusing block,[103] and the equation for the FID deconvolution. In the function, R is the rigid fraction, T_{2R} and T_{2M} are apparent transverse relaxation times of the rigid (hard) and mobile (soft) phase respectively; and *na* is a coefficient that parameterizes the relaxation function.

4.2.3 Hard portion trend

In Figure 4.3 every single dot, plotted as a function of temperature, is a deconvolution of the FID signal measured with TD-NMR at that temperature, which leads to a precise evaluation of the hard portion (R) of the system. Between room temperature and 390 K, where melting occurs for PA, both polymers are solid but above their glass transition temperatures.

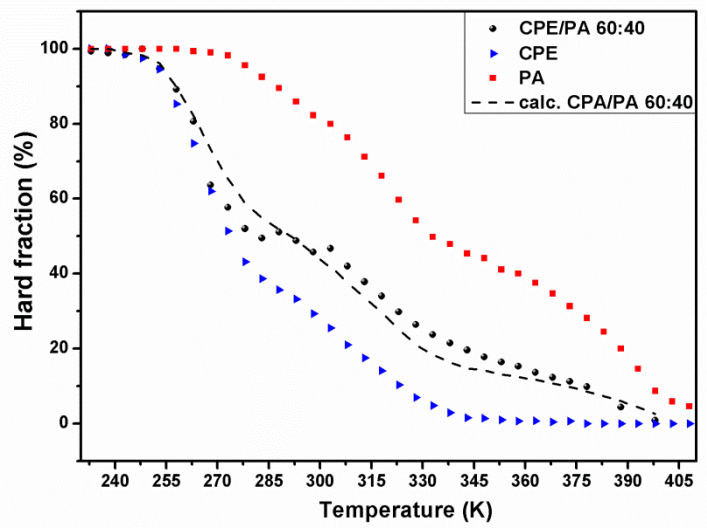

Figure 4.3: Hard fraction percentage, obtained with TD-NMR, of pure CPE, pure PA and CPE/PA 60:40 (w/w) blend is plotted vs. temperature. Solid line is the linear combination of the pure polymers' values.

In this region the values measured for the sample CPE/PA 60:40 (w/w) are quite close to the weighted linear combination of the values for the pure components and this is a strong indicator of phase separation at the microscopic level. However a small deviation reports the effects on the mobility that phases have with each other. Note that at temperature range from 300 to 380 K, that is

the service temperature range, the rigid fraction of the blend is above the weighted average of the two pure components. This is true even if the CPE phase in the blend does not contribute directly to the rigid fraction of the system, as it is completely fluid over 300 K. This phenomenon could be explained with an interaction of the CPE polymer chains with the crystalline phase of the PA that persist at those temperatures. We can assume that any CPE chains associated to rigid PA crystals display a reduced mobility and are then detected as rigid phase from a TD-NMR point of view.

In conclusion, without assuming a real mixing (the two phases are always separated and immiscible), the interfacial interaction are detectable by TD-NMR measurements as a more than proportional increase of rigid fraction in the blend. This proves that the interactions detected by FT-IR technique occur between the amorphous phase of the chlorinated polyethylene and the crystalline phase of the Nylon terpolyamide.

Of course this does not exclude that interfacial interactions may also occur between the amorphous phase of the CPE and the amorphous phase of the PA, that is among the mobile portions. As it was explained before, the Magic Sandwich Echo technique is suitable for the detection of hard phases, for this reason, in the next section will be presented the data collected with a different TD-NMR experiment, the Hahn echo technique, more suitable for the investigation concerning the soft mobile fraction of a system, in the case of CPE/PA blends this will be the amorphous phases over the glass transition temperature.

4.2.4 T_{2m} relaxation times

The following figures indicate the result of the Hahn Echo experiments. In the Hahn Echo experiments, the rigid part described in the previous section is completely invisible, since it is completely relaxed even at short echo times. The

resulting curve of FID intensity as a function of echo time is well fitted by a bimodal exponential decay curve. Each sample is then defined by two T_{2m} values: one, $T_{2m\text{-}FAST}$ that represent the part of the soft portion that relaxes more rapidly and thus has a relatively reduced mobility. This is associated to bulk rubber phase, while the slowest relaxing part, with a relaxation time $T_{2m\text{-}SLOW}$, represents fast moving fractions of the polymer, including chain ends, oligomers, and highly disordered zones with high concentration of defects.

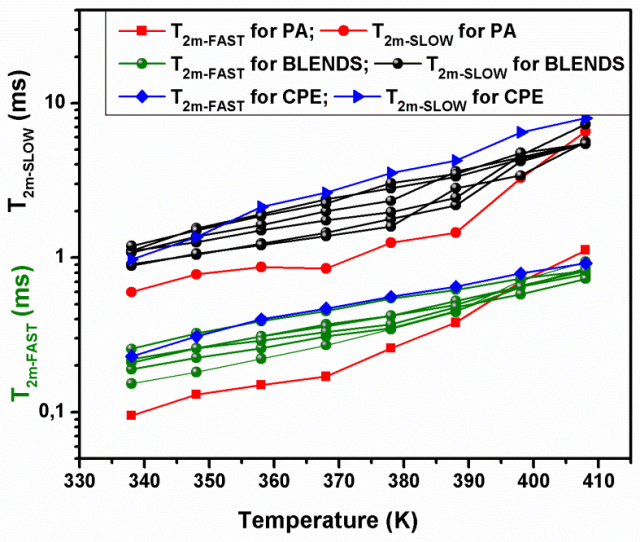

Figure 4.4: $T_{2m\text{-}FAST}$ and $T_{2m\text{-}SLOW}$ for all CPE/PA blends plotted versus the temperature.

Figure 4.4 shows that both 'phases', or portions, for the CPE have a T_2 that evolves approximately as an exponential with temperature. This is stressed by the logarithmic scale, where the CPE appears of course as well fitted by a straight line. The PA has a much different aspect: the T_2 evolves linearly up to 370 K only, and is then steeper. In the CPE there is only the progressive mobilization of the rubber with T, whereas in the PA there is also the melting of crystals. The

result is a catastrophic phenomenon where the increase of T_2 is more than exponential. It has to be noticed that also in this case, the change in measured properties upon changing the blend composition is not linear.

In order to make a more detailed work, all the relevant values were plotted in a series of graphs collected in figure 4.5.

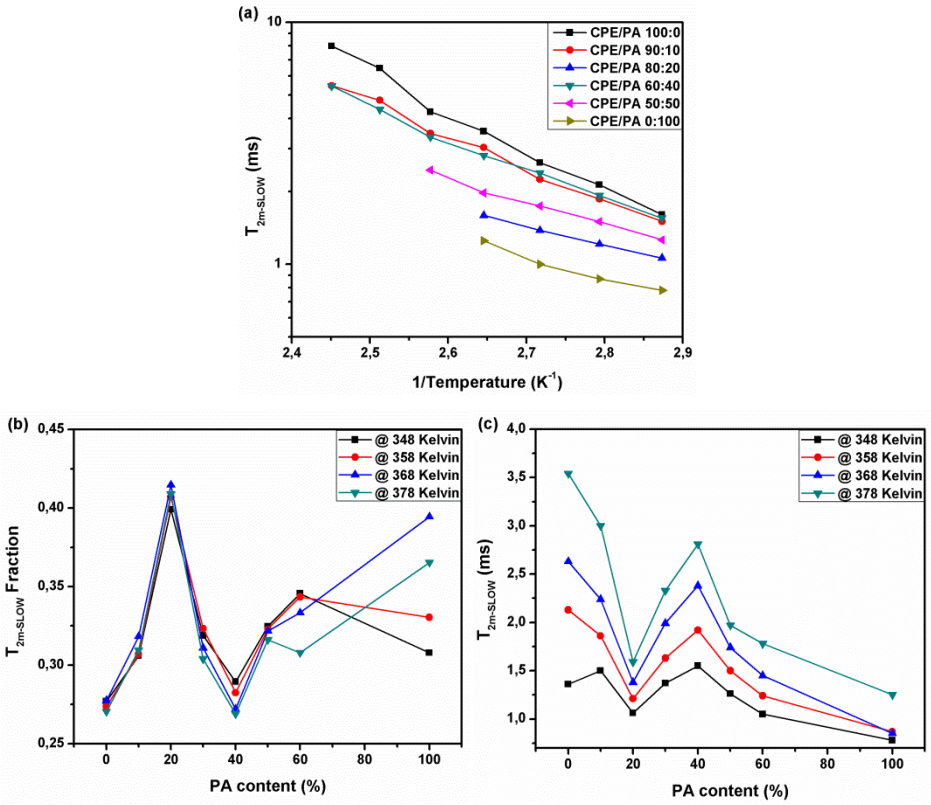

Figure 4.5: a) Arrhenius plot of the $T_{2m\text{-}SLOW}$ as a function of the reciprocal temperature for different CPE/PA compositions. b) Slow fraction (fraction of protons relaxing with $T_{2m\text{-}SLOW}$ in the analyzed bland at a precise temperature) plotted versus Nylon terpolyamide content at different temperatures. c) $T_{2m\text{-}SLOW}$ (in ms) plotted versus Nylon terpolyamide content at different temperatures.

Figure 4.5c describes the temperature evolution of the slow phase (the fast, not shown, is analogous), selecting the points where the PA melting has no discernible effect. From the Arrhenius type plotting we can see that the temperature dependent evolution is linear, indication of a thermally activated process as those present in amorphous polymer phases. The slopes are mostly independent from composition. In the figure one can see that T_2 for CPE/PA 80:20 (w/w) are faster and have more near values to the ones of the pure PA while for CPE/PA 60:40 (w/w) are strangely near to CPE values.

Figure 4.5 a) and b) keep track of the quantity of the two phases as well as measuring their mobility as a function of temperature and composition. The Slow fraction on this range of temperature is practically independent from T in chlorinated polyethylene, and this is a typical behavior for a rubbery material; while, for pure PA there is a strong dependence from T, as the measures register the progressive shrinking of the crystalline phase. Those measures are consistent with those evidenced in Figure 4.5a. A particular, and not expected, behavior, is instead shown by the slow fraction of the blends. With a linear behavior, one could expect that every dot for a CPE/PA composition lies on the straight that combines values of pure components. On the contrary, CPE/PA 80:20 (w/w) blend, at every considered temperatures, lies way above, while CPE/PA 60:40 (w/w) lies below. The immediate interpretation of these data is that 80:20 blend should present a more disordered structure, while 60:40 blend has got a smaller slow-relaxing (i.e. disordered) mobile fraction. CPE/PA 70:30 (w/w) and CPE/PA 50:50 (w/w) blends present an intermediate behavior. Finally, CPE/PA 90:10 (w/w) blend probably evidence that a 10 wt.% of PA is not sufficient to alter CPE properties substantially.

Concurrently, as shown in Figure 4.5c. while the disordered fraction is quantitatively greater, it is also less mobile (CPE/PA 80:20 presents the fastest relaxation times). On the contrary, in the case of CPE/PA 60:40 it is more

mobile, actually approaching the behavior of pure CPE. A deeper speculation of all this data suggest that, as it is mainly the rubbery phase to be seen, this behavior could be related to a continuous CPE phase within the sample, i.e. a co-continuous microstructure for the blend.

In conclusion, even if in 80:20 the PA portion is less, it seems to have an effect on the system as a whole, probably by effects due to high interaction between CPE and PA phases and most likely between the crystalline phase of the PA that somehow "harden" the amorphous phase of the CPE. These effects are minimized in CPE/PA 60:40 (w/w) just because of a finer dispersion and a more structurated morphology that appear to the TD-NMR as a more ordered system.

Further analysis effectuated with Differential Scanning Calorimetry, presented in the next section, will give confirmation of this kind of interaction.

4.3 Crystallization properties of the phases

Polymer blends containing crystallizable components should present a great variety of morphologies.[105] The prediction and control of these morphologies as well as the understanding of the crystallization behavior during its processing will enable enhanced final material properties to be understood.[105] Upon crystallization of a two-component immiscible but compatible blend in which one of them is crystallizable, the crystalline phases separates anyway from the mixtures.[106] This liquid-solid phase separation is different from the liquid-liquid phase separation among the amorphous phases of the two components, and it is vital the understanding where the interfacial interactions occur.

Differential Scanning Chalorimetry (DSC), besides to be one of the most used technique in polymer science, should be the right choice for this kind of investigations.

4.3.1 Experimental

DSC measurements were made with a Mettler Toledo Star^e thermal analysis system equipped with a liquid N_2 low-temperature apparatus, running the experiments under N_2 atmosphere from -50° to 180° C with heating and cooling rates of 10° C/min. The sample weights for the DSC measurements were about 6.5 mg and were measured to an accuracy of 0.05 mg.

4.3.2 Crystallization behavior

The DSC experiments performed in order to understand the crystallizable behavior of the CPE/PA blends in exam were quite peculiar, and aimed, above all, to study and understand the re-crystallization behavior of the two phases in the blend after the melting. Figure 4.6 depicts the thermographs acquired after three scans (heating, cooling and re-heating) for the pure Nylon terpolyamide, and the blends CPE/PA 60:40 (w/w) and CPE/PA 80/20 (w/w), that is, one with a medium content of polyamide in rubber and one with the chlorinated polyethylene as the widely predominant component.

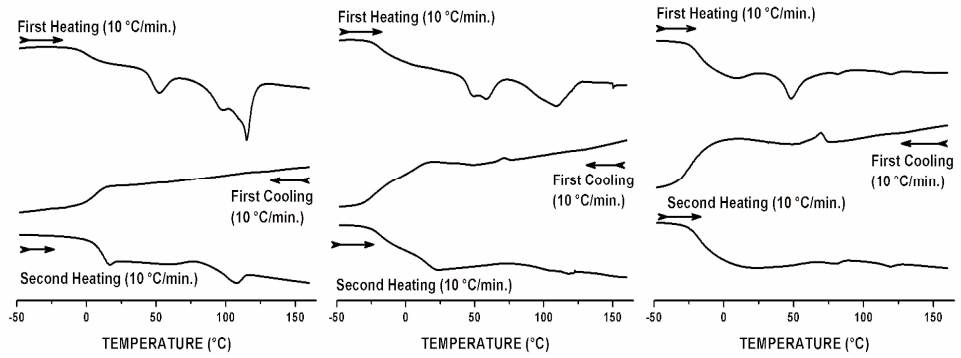

Figure 4.6: Heating-cooling-reheating thermographs for pure PA, CPE/PA 60:40 (w/w) and CPE/PA 80:20 (w/w) blends respectively (from left to right).

The first thing to notice is the small crystallization peaks in the cooling-rate thermographs. For pure PA it is possible to realize that, at the scan speed of the experiment, the polymer do not recrystallize on the cooling. As on the second heating the melting peak appears again, it is clear that the crystallization occurs during heating before the melting of the crystalline phase (i.e. at lower temperatures). By looking at the second and the third graphs, the crystallization peak associated to the polyamide grows evidently and especially in the blend with most CPE phase content. An explanation of this fact should be that the CPE phase in the blend somehow affect and enhance the crystallization of the blended hard thermoplastic phase.

For safer conclusion, other experimets has to be done in order to better understand the nature of the crystalline phases involved, for example Wide Angle X-Ray Diffraction; but these results, combined with the speculation on the relaxometry of the phases obtained with time-domain NMR, let say that interactions between the two phases definitely exist (also confirmed by FTIR analisys) and that the interfacial miscibility occur both between CPE amorphous phase and PA crystalline pahses, and also between the amorphous phases of the two components.

5 Chapter Five: Morphology

In spite of state-of-the-art developments in instrumental techniques, morphology determination of polymer blends remains a formidable challenge. Indeed, methods like light microscopy, scanning electron microscopy, transmission electron microscopy and atomic force microscopy may be used to resolve the polymer blend morphology from the millimeter to the sub-nanometer scale, but they image only the surface of the materials and rarely provide information on the internal (bulk) structure.

However, understanding the structure-properties relationship in thermoplastic elastomers from elastomer / hard thermoplastic simple blends is vital for making blends with tailored properties. In this chapter the most outstanding results of the whole thesis work will be presented, and also the path that led to the idea that allowed to directly visualize the three-dimensional microstructure of the materials in exam.

5.1 Surface scanning

Even though it is mainly able to scan only the surface of a material in exam, atomic force microscopy (AFM) is a powerful technique widely used in the literature for mapping the morphology of polymer blends; especially nanoindentation and Tapping Mode AFM (TMAFM) imaging techniques are used as experimental tools.[107]

5.1.1 Experimental

Samples for Atomic Force Microscopy have been prepared by manual die cutting cubes of c.a. 2 x 4 x 3 mm from the samples obtained by injection molding; and compressed a little bit in order to flatten the surface (about 5% in the z direction for 300 seconds at 90° C, between glass slices). The roughness of the surface was scanned with a profilometer in four directions (45°, 90°, 135° and 180° angles; with length of 1 mm and speed of 0.02 mm/sec) in order to put samples flat enough to really visualize the phase separations of the phases in the samples. Too rough specimens were flattened again until a final maximum roughness of less that 300 nm.

Tapping Mode Atomic Force Microscopy (TMAFM) studies were carried out with the aid of a NanoScope III-M system (Digital Instruments, Santa Barbara, CA), equipped with a J-type vertical engage scanner. TMAFM observations were performed at room temperature in air using silicon cantilevers with nominal spring constant of 40 N/m and nominal resonanc frequency of 300 kHz (standard silicon TESP probes).

5.1.2 AFM images of the surface

Figure 5.1 shows a two-dimensional topographic image (left) along with the corresponding phase image (right) for the CPE/PA 60:40 (w/w) blend specimen, as it is the material with the most intriguing mechanical and rheological properties, obtained by TMAFM. The magnification of these images is indicated by the scan dimension, which is 20 μm. The topographic image shows continuous structures of darker color surrounded by continuous region of brighter color. Already from this analysis, given that it was demonstrated (see DMA results in chapter three) that this blend behave like a phase separated system, is it clear that two different phases can be distinguished. Like the topographic image, the phase image has continuous structures of darker colour surrounded by relatively uniform continuous bright color.

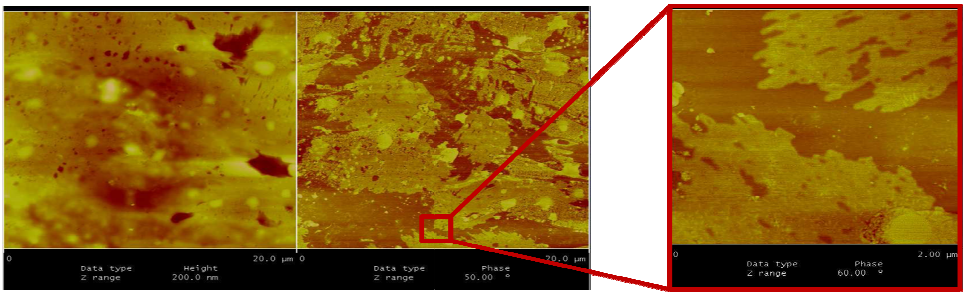

Figure 5.1: Tapping mode AFM topographic image (left) and phase image (center) of the flattened surface of the CPE/PA 60/40 (w/w). Color contrast from dark to bright represents a total range of 200 nm in height image and 50° in phase image. The image on the right is a scan in the zoomed region indicated in the picture, and it is a phase image with a z-range of 60°.

A zoomed image of a region of 2 x 2 μm is also depicted, highlighting the phase separation within the sample.

Without further analysis, positive identification of the dark or bright region in the phase image in Figure5.1 as CPE or PA phase is not possible. Even in the literature it is not really clear if, for example, the darker region, correspond to the less stiff[108,109,110] or to the stiffer[111,112,113] material.

Furthermore, it is easily possible that the preparation of the specimens, i.e. the flattening between glassy slices, could have affected the morphology and the phases distribution in the material. Finally, it is not obvious that the material in the bulk would behave as in the surface.

The next two section of this chapter, dedicated to the morphological study of the CPE/PA blends will give more detailed and precise results concerning the microstructure of the samples.

5.2 More in depth...

Investigation of the morphology of an immiscible polymer blend by means of Scanning Electron microscopy (SEM), is by far the most widely used.[65,114,115,116] The most common way to study the blend morphology close to the sample surface is to remove (e.g. by selectively dissolving) one of the polymers and then use electron microscopy to visualize the resulting grooves. These kind of techniques are often used for the detection of co-continuous structures in polymer blends, in particular after extraction of one phase that lasts several hours. Indeed, in the present case, it was chosen for the etching process to extract PA only in proximity of the surface since the complete removal of the hard phase from the specimen would lead to the collapse of the CPE matrix.

5.2.1 Experimental

Cubes of c.a. 2 x 4 x 3 mm were manual die cut from the samples obtained by injection molding and compressed a little bit in order to flatten the surface (about 5% in the z direction for 300 seconds at 90° C, between glass slices). A drop of pure acetic acid has been put on the specimens' surface for few seconds at room temperature before pouring them in water and drying at 50° C for two hours. The treated surface was than directly observed with SEM without coating.

Scanning electron microscopy (SEM) images were obtained with a low voltage LEO 1530 instrument.

5.2.2 SEM micrographs after surface etching

In Figure 5.2**,** some scanning electron images of 60:40 (w/w) CPE/PA blend are reported.

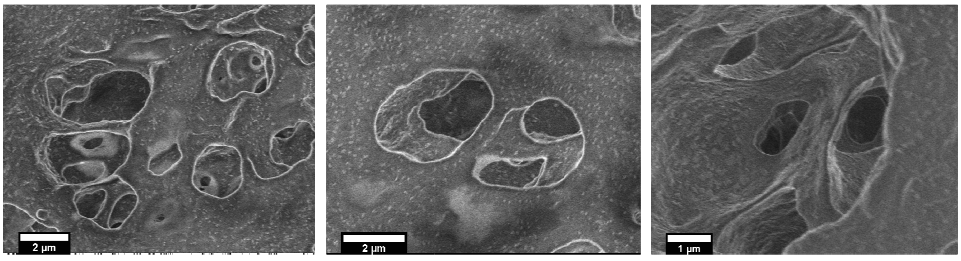

Figure 5.2: SEM micrographs at different magnifications of 60:40 (w/w) CPE/PA blend after removal of the PA portion by surface treatment

The SEM images were obtained after surface treatment with formic acid, which enabled the removal of the polyamide only. Micrographs show the presence of quasi-spherical voids interconnected one with the others, the weave of these empty spaces suggests the existence of a three-dimensional network

comparable of a co-continuous structure suggested also in the TMAFM images of the same blend, but with, in addiction, a slightly greater depth of field.

Scanning Electron Microscopy technique is definitely more precise, in this respect, for the morphological investigation of the blends. Anyhow, also in this case, the treatment done over the specimens may have affected the final results, and, despite the depth of field, the bulk of the material has not yet been displayed.

In the next, and last section of this chapter, a new technique for the direct visualization of the inner structure of thermoplastic elastomer blend via a facile and non-chemical labeling processing of one phase selectively will be presented.

5.3 The bulk microstructure

Laser Scanning Confocal Fluorescence Microscopy (LSCFM) is a method commonly used in cell biology to obtain information for the structure and morphology of living cells with depth selectivity.[117] The key feature of confocal microscopy is its ability to acquire in-focus images from selected depths, a process known as optical sectioning. Images are acquired slice-by-slice and reconstructed with a computer, allowing three-dimensional visualization of topologically complex objects.[118]

After the seminal work of Verhoogt et al. in the use of reflection mode laser scanning confocal microscopy (LSCM) to visualize polymer blends,[68] several studies have been reported in literature. In particular Jinnai and co-workers have extensively utilized LSCM to visualize co-continuous structures generated during the late stage of spinodal decomposition of binary mixtures of deuterated polybutadiene/polybutadiene and of poly(styrene-ran-butadiene)/polybutadiene.[69] More recently has been reported that a covalent-labeling of one of the polymer components with a fluorescent dye may enable the possibility to characterize the

internal microscopic structure of phase separated polymer blends through laser scanning confocal fluorescence microscopy (LSCFM).

In the present thesis work, a well defined three-dimensional experimental image will be presented for a thermoplastic elastomer based on a rubber/plastic blend with continuous interpenetrating phases, by means of the laser scanning confocal fluorescence microscopy. Furthermore, the observed changes in the morphology upon tuning the rubber/plastic ratio were clearly related to the changes in the mechanical properties of the blends.

5.3.1 Experimental

With the aim of labeling the CPE rubber with a dye, thin films were prepared by solution casting from a $5x10^{-7}$ M solution of a fluorescent dye in THF with 10 vol. % of CPE rubber inside (so the final concentration of the dye in CPE was $5x10^{-6}$M). The florescent dye used to label the CPE is N,N'-Bis-(1-Heptyloctyl)-perylene-3,4:9,10-tetracarboxidiimide (PDI) synthesized and purified as described elsewhere.[119] Its chemical structure is reported below; the choice fell on this type of molecule because of its extremely high quantum yield of fluorescence, its tendency to dissolve in chlorinated solvents (mainly due to the alkyl substituent on the nitrogens) and its proficient photostability.

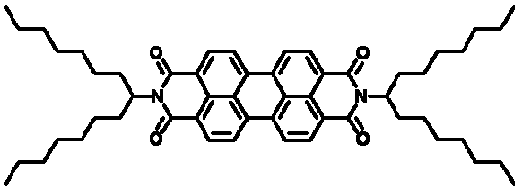

Before blending with the hard thermoplastic, the obtained labeled-CPE thick films (of ca. 30 μm) were all analyzed by means of LSCFM in, at least, 6 different region, with the aim to check the homogeneous dispersion of the PDI dye in the rubber. Figure 5.3 depicts this homogeneous distribution of the dye, at

least in the micrometer scale. Figure 5.3 b is acquired after 30-40 seconds of exposure of the sample at the maximum power of the laser that photo-bleached the dye.

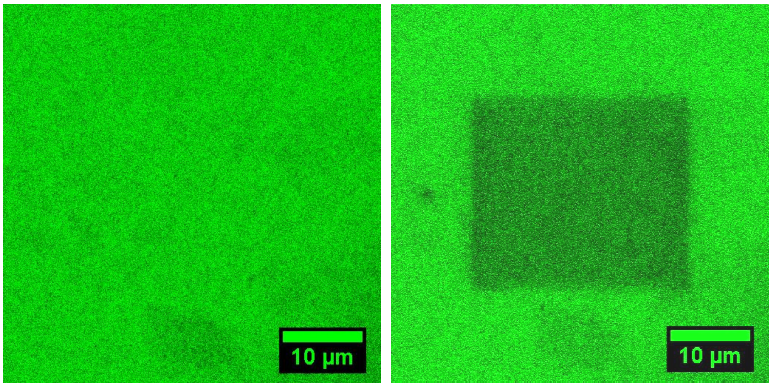

Figure 5.3: LSCFM images of the pure CPE after solution treatment with PDI dye. On the left it is possible to see the uniformly distribution of the dye in the rubbery phase. On the right, dark square region is due to the effect of photo-bleaching with the laser.

Four blends of so obtained labeled CPE and pure polyamide were compounded with a DSM µ-processing internal mixer having a 5 ml volume chamber with CPE/PA ratios of 80:20, 60:40 and 40:60 by weight. Note that the reduced volume was needed for the labeling. Blending was allowed to proceed for 420 seconds at a temperature of 150° C and 80 rpm rotor speed. Specimens were taken as came out from the extruder, without any treatment, immersed in oil with a high refractive index and observed by means of LSCFM technique.

5.3.2 2D Images of the bulk and 3D reconstruction

In order to enable LSCFM for studying CPE/PA blends morphology, one of the components should be fluorescently labeled. To this end, three additional samples with CPE/PA ratios 80:20, 60:40 and 40:60 (w/w), corresponding to soft, elastic and plastic materials were prepared. Before the blending of these samples with the internal mixer, the CPE was labeled with a fluorescent dye by simple solution treatment as described in the experimental section, checking the homogeneity of the dispersion of the dye within CPE by means of LSCFM. For each blend, series of images (z-stacks) were then obtained by continuously shifting the microscope focus deeper into the sample, up to ~70 μm depth. The number of images in a z-stack was defined by the distance between each successive focal plane, typically between 0.3 and 0.4 μm. With those images, three dimensional reconstruction of the morphology of the blends were prepared. Figure 5.4 depicts for each blend: an example of original image acquired by the microscope; a three-dimensional image reconstruction in which the fluorescent CPE phase is shown in green and the non fluorescent PA phase in black; a three-dimensional binarized[120] image with fluorescent CPE shown in white.

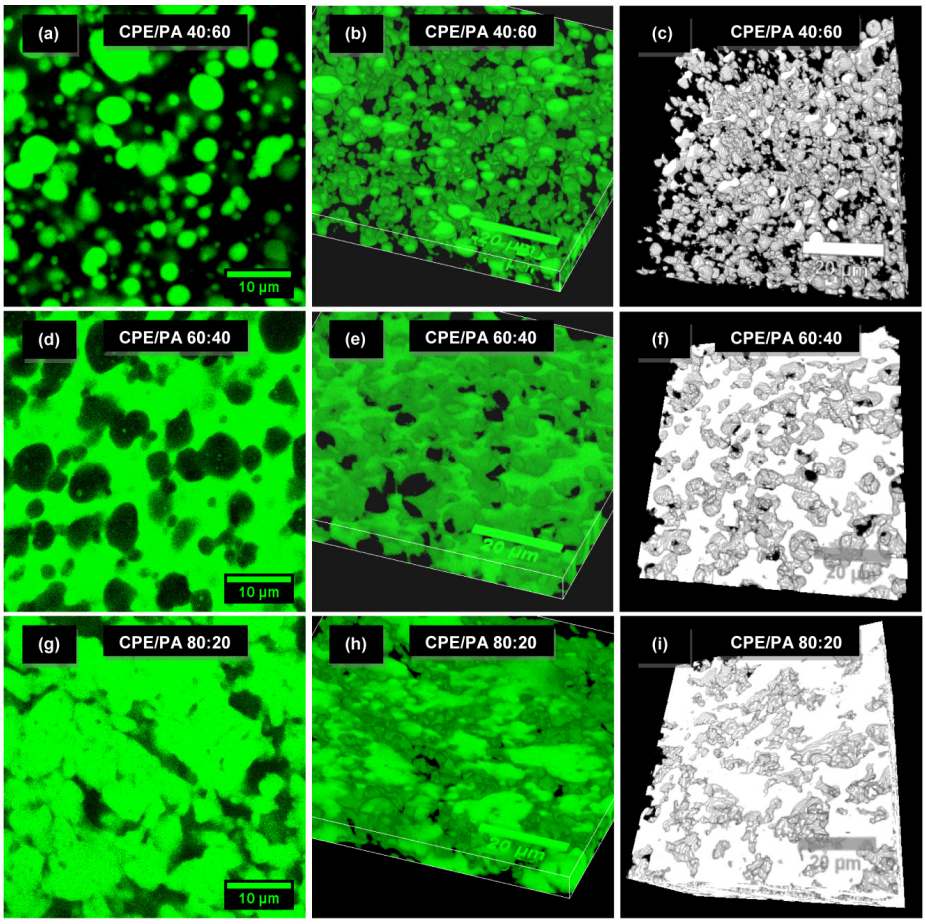

Figure 5.4: (a) (d) (g) sliced 2D LSCFM images of CPE/PA blends (CPE in green, scale bars 10 µm). (b) (e) (h) 3D images constructed by a series of sliced 2D LSCFM images of CPE/PA blends (CPE in green, scale bars 20 µm). (c) (f) (i) 3D images reconstructed by binarized 2D LSCFM images of CPE/PA blends (CPE in white, scale bars 20 µm).

The images display morphologies consistent with the mechanical behavior of the respective CPE/PA blends, as evidenced in details in Figure 5.5.

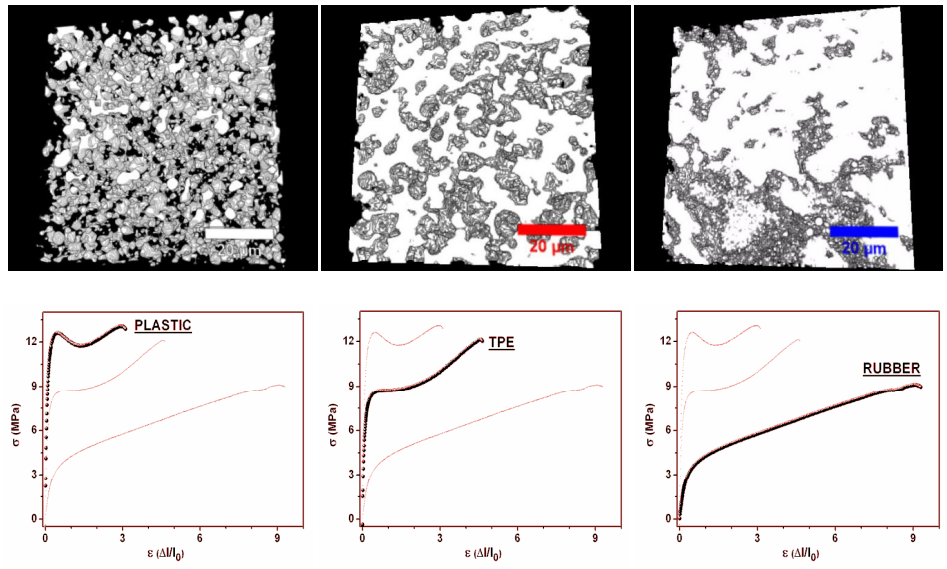

Figure 5.5: The bulk three-dimensional structures presented above are here correlated with a precise macroscopic mechanical behavior: dispersed spheres of CPE in PA matrix match with a typical thermoplastic behavior (a and d); the co-continuous structure present a stress-strain curve of a vulcanized rubber, i.e. a thermoplastic elastomer (b and e); disordered PA phase dispersed in CPE behave like a un-vulcanized rubber.

For the 40:60 (w/w) CPE/PA blend in Figure 5.4 (a-c) the rubbery phase is observed discretely dispersed in the plastic. The final properties of the bulk material would then be one of a plastic, with a narrow yield point and a typical plastic deformation plateau. The structure highlighted in Figure 5.4 (d-f) instead, corresponding to the 60:40 (w/w) blend, is the most intriguing concerning its microscopic structure. Here the rubbery and the hard thermoplastic phases are continuous and interpenetrating, so they lead to final tensile properties comparable to those of a vulcanized rubber, that is, a thermoplastic elastomer blend. As expected, the improved mechanical properties are then due to a co-continuous structure. In Figure 5.4 (g-i) LSCFM images of CPE/PA 80:20 (w/w)

are reported. In this blend the rubbery phase is the most abundant and the hard phase is disorderly dispersed in it. This means that a stress-strain curve should coincide to that of a raw rubber, as demonstrated in the previous section.

The separation length scale between phases, either in case of spheres or open-foam like structure, is comparable and in the order of 2-5 microns. This indicates a good mixing process and is consistent with the enhanced mechanical macroscopic properties. Furthermore, as clarified by Figure 5.6, the phase separation length scale revealed through LSCFM reconstruction is comparable with the one obtained by means of scanning Electron Microscopy, and thou strengthens the data collected with that technique.

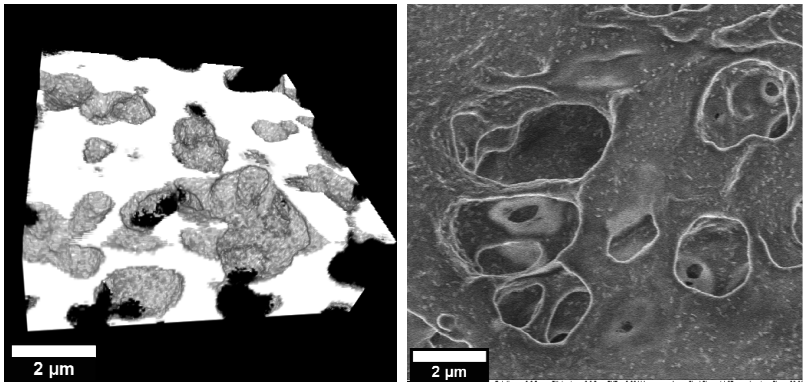

Figure 5.6: (a) LSCFM image of the morphology of sample CPE (labeled)/PA 60:40 (w/w). The image is a 3D reconstruction after a z-scan of 8 µm, brighter parts are fluorescent CPE. (b) SEM micrograph of sample CPE/PA 60:40 (w/w) after removal of PA by surface treatment.

Most of the results presented in this chapter has been recently published.[121]

Conclusions

At appropriate compositions chlorinated polyethylene and Nylon -6/-(6,6)/-12 terpolyamide were found to be compatible and formed blends with the characteristics of thermoplastic elastomers, as revealed by thermo-mechanical studies. Thus, thermoplastic elastomeric materials with enhanced mechanical characteristics were obtained without need of compatibilizer.

ATR-FTIR allowed the detection of a small number of weak interactions among amide groups of Nylon and chorines of CPE that have been related to the partial miscibility and thus compatibility between the two separated phases of the immiscible blends. DSC measurements give evidence that interfacial interactions occur also between the amorphous phase of the CPE and the crystalline phase of the PA.

^{1}H TD-NMR gave a comprehensive view of the materials in terms of polymer chain mobility. Combined Hahn Echo and MSE measurements indicate that in the blends the two phases are separated and their rigid fractions evolve almost independently, except for a minor amount within the service temperature range of the materials, demonstrating the interactions detected by DSC. On the other side, the interaction between mobile phases is also characterized, as if the vast interface present in micro phase separated fractions is sufficient to cause an averaging of chain mobility, even without intimate blending.

The morphology of these materials was studied by laser scanning confocal fluorescence microscopy (LSCFM) and a unique co-continuous structure responsible for the improved mechanical properties of the 60:40 (w/w) CPE/PA blend was revealed.

The experimental investigations on the morphology showed that LSCFM is a powerful tool for the examination of the microstructure of the blends giving excellent image contrast and sub-micrometer resolution. Using this method the 3D morphology of a thermoplastic elastomer from a rubber/plastic binary blend was directly visualized for the first time giving important evidence for the strong correlation between the microscopic structure and the macroscopic properties of these materials.

ACKNOWLEDGMENTS

This work was supported by the IMPRS program from the Max Plank Gesellschaft, and by the Fondazione Cariplo at the University of Milano Bicocca.

First, I would like to thank Dr. Roberto Simonutti for his guidance during these last three years. Not less, I have to thank Dr. Claudio Rebuscini and Dr. Gilda De Luca for the initial motivation to this PhD route.

I am also very thankful to Prof. Dr. Hans-Jürgen Butt and Dr. Kaloian Koynov from the Max Plank Institute for Polymer Research for hosting me in my abroad period there, for being friendly but guiding, and especially for allowing me to reach the most outstanding results in my PhD studies. I definitely have to thank as well all the people in MPI-P in Mainz for the enjoyable period that I spent there. I would like also to acknowledge all the people I collaborated with, and who helped me in the realization of the work presented in this dissertation.

A dear thank goes to Michele Mauri (and his indispensable electric heater), Lucio Mauri, Luca De Trizio, Annalisa Colombo and all the guys and girls that contributed to make U5 a nice and stimulating workplace.

I gladly thank my family for their inexhaustible patience, for believing in me and for driving me to reach this, last, important milestone.

Very special thanks goes to that fellowship of friends known, since TEN years, as GCS. Particular and sincere acknowledgments to Dr. Alberto *Brodo* Bianchi for his amazing way to be a Hobbit, to Dr. Claudio *Dino* Somaschini for having recently introduced the MagaSkyping experience and to Dr. Glauco *Tone* Battagliarin for the 'Midnights in Mainz'.

Last, and most significant, thanks to the person that drives me every day to give the best of myself. Grazie Ramo!

REFERENCES

[1] G. Holden in "Understanding thermoplastic elastomers". Hanser Publishers, Munich, Germany (2000).

[2] R. Costa, N. K. Dutta, N. R. Choundry, A. K. Bhowmick in "Current topics in Elastomer research" A. Bhowmick, CRC Press, Boca Raton, USA (2008) cap. 5 "Thermoplasic Elastomers".

[3] N. R. Legge, G. Holden, H. E. Schröder in "Thermoplastic elastomers. A comprehensive rewiew". Hanser Publishers, Munich, Germany (1987).

[4] G. Holden, E. T. Bishop, N. R. Legge. *J Polym Sci, Polym Symp* 26 (1969) 37-57.

[5] S. K. De, A. K. Bhowmick in "Thermoplastic Elastomers from Rubber-Plastic Blends". Ellis Horwood Ltd., New York, USA (1991).

[6] H. Pernot, M. Baumert, F. Court, L. Leibler, *Nat Mater*, 1 (2002) 54.

[7] J. G. Drobny in "Handbook of Thermoplastic Elastomers", William Andrew Inc., New York, USA (2007).

[8] Y. Furakawa, Inventing Polymer Sceince, University of Pennsylvania Press, Philadelphia, USA, (1998).

[9] N. R. Legge, G. Holden, H. E. Schröder in "Thermoplastic elastomers. A comprehensive rewiew". Hanser Publishers, Munich, Germany (1987) cap.1.

[10] Bailey J. T., Bishop E. T., Hendricks W. R., Holden G., Legge N. R.; *Rubber Age*, (1966), 98, 69.

[11] A. Y. Coran, R. Patel; *Rubb Chem Technol*; 53 (1980) 141 .

[12] A. Y. Coran, R. Patel; *Rubb Chem Technol*; 53 (1980) 781.

[13] A. Y. Coran, R. Patel; *Rubb Chem Technol*; 54 (1981) 91.

[14] A. Y. Coran, R. Patel; *Rubb Chem Technol*; 54 (1981) 892.

[15] A. Y. Coran, R. Patel, D. Williams; *Rubb Chem Technol*; 55 (1982) 116.

[16] A. Y. Coran, R. Patel, D. Williams; *Rubb Chem Technol*; 55 (1982) 1063.

[17] A. Y. Coran, R. Patel; *Rubb Chem Technol*; 56 (1983) 210.

[18] A. Y. Coran, R. Patel; *Rubb Chem Technol*; 56 (1983) 1045.

[19] A. Y. Coran, R. Patel, D. Williams; *Rubb Chem Technol*; 58 (1985) 1014.

[20] J. R. Wolfe in "Thermoplastic elastomers. A comprehensive rewiew". Hanser Publishers, Munich, Germany (1987). Cap.6.

[21] P. J. Flory, A. Abe; *Macromolecules*, 11 (1978) 1119.

[22] F. S. Bates, G. H. Fredrickson; *Phys Today*, 52 (1999) 32.

[23] F. S. Bates, G. H. Fredrickson in "Thermoplastic Elastomers" 3rd edition, Chapter 15, (G. Holden, H. R. Kricheldorf, R. P. Quirk), Hanser Publisher, Munich, Germany, (2004)

[24] P. Bahadur; *Current Science*, 80 (2001) 1002.

[25] T. Hashimoto, A. Todo, H. Itoi, H. Kaway; *Macromolecules*, 10 (1977) 377.

[26] R. N. Choundry, A. K. Bhowmick; *J Adhes Sci Technol*, 2 (1988) 167.

[27] R. N. Choundry, A. K. Bhowmick; *J Adhes Sci Technol*, 1 (1990) 27.

[28] S. Wu, in "Polymer Interface and Adhesion", Marcel Dekker Inc., New York, (1982).

[29] R. Frenkel, V. Duchacek, T. Kirillova, E. Kuz'min, *J Appl Polym Sci*, 34 (1987) 1301.

[30] W. K. Witsiepe, *Adv Chem Ser,* 129 (1973) 39.

[31] A. A. Apostolov, S. Fakirov; *J Macromol Sci, Phys B*, 31 (1992) 329.

[32] J. D. Tong, R. Jerome, *Macromolecules*, 33 (2000) 1479.

[33] B. Pukànszjy, *Eur Polym J*, 41 (2005) 645.

[34] E. Pedemonte, G. C. Alfonso, G. Dondero, C. F. De, L. Araimo; *Polymer*, 18 (1977) 191.

[35] H. T. Ban, T. Kase, M. Kawabe, A. Miyazawa, T. Ishihara, H. Hagihara, Y. Tsunogae, M. Murata, T. Shiono; *Macromolecules* 39 (2006) 171.

[36] R. N. Choundry, A. K. Bhowmick; *J Mater Sci*, 25 (1990) 161.

[37] N. R. Choundry, T. K. Chaki, A. Dutta, A. K. Bhowmick; *Polymer*, 30 (1989), 2047.

[38] R. P. Quirk, M. Morton in "Thermoplastic Elastomers, 2nd ed.., G. Holden, N. R. Legge, R. P. Quirk, H. E. Shroeder, Hanser Publisher, New York, USA (1996), Chapter 4.

[39] J. P. Kennedy in "Thermoplastic Elastomers, 2nd ed.., G. Holden, N. R. Legge, R. P. Quirk, H. E. Shroeder, Hanser Publisher, New York, USA (1996), Chapter 13.

[40] L. K. Bi, L. J. Fetters; *Macromolecules*, 8 (1975) 98.

[41] F. S. Bates, G. H. Fredrickson in "Handbook of Thermoplastic Elastomers" 2nd ed., B. M. Walker, C. P. Rader Eds., Van Nostrand Reinhold, New York, USA (1998), Chapter 12.

[42] K. Matyjaszewski, J. Xia; *Chem Rev*, 101 (2001) 2921.

[43] J. Chiefari, Y. K. Chong, F. Ercole, J. Krstina, J. Jeffery, T. P. T. Le, R. T. A. Mayadunne, G. F. Meijs, C. L. Moad, G. Moad, E. Rizzardo, S. H. Thang; *Macromolecules*, 31 (1998) 5559.

[44] B. Dufour, K. Koynov, T. Pakula, K. Matyjaszewski, *Macromol Chem Phys*, 209 (1998) 1686.

[45] A. Juhari, J. Mosnàcek, J. A. Joon, A. Nese, K. Koynov, T. Kowalewski, K. Matyjaszewski; *Polymer*, 51 (2010) 4806.

[46] W. J. McKnoght, R. D. Lundberg in Chapter 10 of "Thermoplastic Elastomers", 2nd ed., G. Holden, N. R. Legge, R. P. Quirk, H. E. Shroeder, Hanser Publisher, New York, USA (1996).

[47] J. C. Falk, D. A. Van Beck; U. S. Patent 4,473,679 (1984).

[48] PAC, 2007, 79, 1801. Definitions of terms relating to the structure and processing of sols, gels, networks, and inorganic-organic hybrid materials (IUPAC Recommendations 2007), doi:10.1351/pac200779101801.

[49] W. P. Gergen, in Chapter 11 of "Thermoplastic Elastomers", 2nd ed.., G. Holden, N. R. Legge, R. P. Quirk, H. E. Shroeder, Hanser Publisher, New York, USA (1996).

[50] D. R. Paul, J. W. Barlow, *Advances in Chem Series*, 211 (1986) 3.

[51] N. Kinsuk, *Rubber Chem Technol*, 80 (2007) 504.

[52] R. A. Emmett, *Ind Eng Chem*, 36 (1944) 730.

[53] E. Badum, U. S. Patent 2,297,194 (1942).

[54] A. Ibrahim, M. Dahlan, *Prog Polym Sci*, 23, (1998) 665.

[55] P. Poetschke, D. R. Paul; *J Macromol Sci; C: Pol Rev*, 43 (2003) 87.

[56] L. A. Utraky in "Commercial Polymer Blends", Chapman et. Hall, London, U. K. (1998).

[57] L. A. Utraki in Morphology in "Commarcial Polymer Blends", Chapman et. Hall, London, U. K. (1998).

[58] L. A. Utraki in "Polymer Alloys and Blends: Thermodynamics and Rheology", Hanser Publ, Munchen, Germany (1989).

[59] D. R. Paul, S. Newman in "Polymer Blends", Academic Press, New York, U. S. A., (1978).

[60] A. Mamat, T. Vu-Khan, P. Cigana, B. D. Favis; *J Polym Sci, B: Polym Phys*, 35 (1977) 2583.

[61] U. Niebergall, J. Bohse, S. Seidler, W. Grellmann, B. L. Schurmann, *Polym Eng Sci*, 39 (1999), 1109.

[62] P. Poetschke, D. R. Paul; *J Macromol Sci; C: Pol Rev*, 43 (2003) pag. 103.

[63] B. Watts, C. R. McNeill, *Macromol. Rapid Commun.* 31 (2010) 1706.

[64] H. Janik, B. Pałys, Z. S. Petrovic, *Macromol. Rapid Commun.* 24 (2003) 265.

[65] C. Nakason, S. Jamjinno, A. Kaesaman, S. Kiatkamjornwong, *Polym Adv Technol* 19 (2008) 85.

[66] P. Sengupta, J. W. M. Noordermeer, *Polymer* 46 (2005) 12298.

[67] P. Sengupta, J. W. M. Noordermeer, *Macromol. Rapid Commun.* 26 (2005) 542.

[68] H. Verhoogt, J. V. Dam, A. P. de Boer, A. Draaijer, P. M. Houpt, *Polymer* 34 (1993) 1325.

[69] H. Jinnai, Y. Nishikawa, T. Ikehara, T. Nishi, *Adv. Polym. Sci.* 170 (2004) 115.

[70] K. Deng, N. Felorzabihi, M. A. Winnik, Z. Jiang, Z. Yin, P. V. Yaneff, R. A. Ryntz, *Polym. Advan. Technol.* 20 (2009) 235.

[71] C. R. López-Barrón, C. W. Macosko, *J. Microscopy* 242 (2011) 242.

[72] C. R. López-Barrón, C. W. Macosko, *Langmuir* 26 (2010) 14284.

[73] J. Li, B. D. Favis, *Polymer*, 42 (2001) 5047.

[74] C. N. Bunnell, R. H. Parry; *Appl Polym Symp*, 11 (1969) 95.

[75] J. kroshwite, H. F. March, N. M. Gaylord in "Encyclopedia of Polymer Science and Technology. Polyethylene Compounds", John Wiley and Son's, New York, U. S. A. (1985), p 495.

[76] W. Nishimoto, K. B. Sinclair in "Chlorinated Polyethylene"SRI International No. 83, Stanford Research Institute, Menlo Park, CA, U. S. A. (1984).

[77] J. C. Salamone in "Polymeric Material Encyclopedia, CRC Press, Boca Raton, FL, U. S. A. (1996) p 1235.

[78] A. moradi, A. S. A. Ramazani, M. Shahrokhi, *Polym J*, 37 (2005) 661.

[79] R. G. Alamo, K. Jeon, R. L. Smith, E. Boz, K. B. Wagener, M. R. Bockstaller, *Macromolecules*, 41 (2008) 7141.

[80] S. Stoeva, A. Popov, R. Rodriguez, *Polymer*, 45 (2004) 6341.

[81] S. Stoeva, K. Gjurova, M. Zagorcheva, *Polym. Degrad. Stabil.* 67 (2000) 117.

[82] M. C. Elisa, T. J. McCarthy, Macromolecules, 25 (1992) 2603.

[83] S. Stoeva, *J Appl Polym Sci*, 101 (2006) 2602.

[84] X. Liu, H. Huang, Y. Zhang, Y. Zhang, *J Appl Polym Sci*, 89 (2003) 1727.

[85] H. Huang, X. Liu, T. Ikehara, T. Nishi, *J Appl Polym Sci*, 90 (2003) 824.

[86] K. Marchildon, *Macromol Reaction Eng*, 5 (2011) 22.

[87] M. Avella, E. Martuscelli, M. Raimo, *J. Mater. Sci.* 35 (2000) 523.

[88] DuPont™ Elvamide ® Product and Properties Giude (http://plastics.dupont.com/plastics/pdflit/americas/elvamide/ELVPPe.pdf).

[89] D. D. Rudolph, S. A. Orroth, R. I. Bhagat, *Polym plast technol Eng*, 29 (1990) 289.

[90] K. Venkataswamy, Paper Presented at the Conference TPE 2011, Brusselles, Belgium, November 8th – November 9th 2011.

[91] P. Ellis, Paper Presented at the Conference TPE 2011, Brusselles, Belgium, November 8th – November 9th 2011.

[92] S. Kar, P. K. Maji, A. K. Bhowmick, *J Mater Sci*, 45 (2010) 64.

[93] L. Wang, Z. Zhang, H. Chen, S. Zhang, C. Xiong, *J. Polym. Res.*17 (2010) 77.

[94] C. H. Stephens, H. Yang, M. Islam, S. P. Chum, S. J. Rowan, A. hiltner, E. Baer, *J Pol Phys, B: Polym Phys*, 41 (2003) 2062.

[95] G. Martinez, J. Millan, J. Contreras, *J Polym Sci, A: Pol Chem*, 41 (2003) 508.

[96] J. Sullivan, *Comp Sci Technol*, 39 (1990) 207.

[97] E. T. Kopesky, T. S. Haddad, G. H. McKinley, R. E. Cohen, *Polymer* 46 (2005) 4743.

[98] J. Cañavate, P. Pages, J. Saurina, X. Colom, F. Carrasco, *Polym Bull*, 44 (2000) 293.

[99] H. Huang, S. Malkov, M. Coleman, P. Painter, *Macromolecules,* 36 (2003) 8148.

[100] H. Huang, S. Malkov, M. Coleman, P. Painter, *Macromolecules,* 36 (2003) 8156.

[101] A. Abragam in "Principles of Nuclear Magnetism", Oxford University Press, Oxford, 1983.

[102] W. S. Price, *Conc Magnetic Res*, 9 (1997) 299.

[103] A. Maus, C. Hertlein, K. Saalwächter; *Macromol Chem Phys* 207 (2006) 1150.

[104] M Mauri, Y. Thomann, H. Shneider, K. Saalwächter, *Solid State nucl Magn Reson*, 34 (2008) 125

[105] T. S. Plivelic, S. N. Cassu, M. C. Goncalves, I. L. Torriani; *Macromolecules*, 40 (2007) 253.

[106] D. Debier, A. M. Jonas, R. Legras, *J Polym Sci B: Polym Phys*, 36 (1998) 2197.

[107] P. Achalla, J. McCormick, T. Hodge, C. Moreland, P. Esnault, A. Karim, D. Raghavan, *J Polym Sci B: Polym Phys*, 44 (2006) 492.

[108] R. S. McLean, B. B. Sauer, *Macromolecules*, 30 (1998) 8314.

[109] S. N. Magonov, V. Ellings, M. H. Whangho, *Surf Sci*, 375 (1997) 385.

[110] F. Clement, A. Lapra, L. Bokobza, L. Monnerie, P. Menez, *Polymer*, 42 (2001) 6259.

[111] G. Bar, Y. Thomann, R. Brandsch, H. J. Cantow, M. H. Whangho, *Langmuir*, 14 (1998) 1219.

[112] B. B. Sauer, R. S. McLean, R. R. Thomas, *Langmuir*, 14 (1998) 3045.

[113] S. N. Magonov, V. Ellings, V. S. Pakov, *Polymer*, 38 (1997) 297.

[114] R. T. Tol, G. Groeninckx, I. Vinckier, P. Moldenaers, J. Mewis, *Polymer* 45 (2004) 2587.

[115] W. Pechurai, C. Nakason , K. Sahakaro, *Polym Test*, 27 (2008) 621.

[116] W. Yu, W. Zhou, C. Zhou, *Polymer*, 51 (2010) 2091.

[117] J. B. Pawley, *Handbook of Biological Confocal Microscopy*, 3rd edition, Springer, Berlin, Germany **2006**, cap. 19.

[118] M. Moffitt, Y. Rharbi, H. Li, M. A. Winnik, *Macromolecules* 35 (2002) 3321.

[119] F. Nolde, W. Pisula, S. Müller, C. Kohl, K. Müllen, *Chem Mater*, 18 (2006) 3715

[120] Y. Hirokawa, T. Okamoto, K. Kimishima, H. Jinnai, S. Koizumi, K. Aizawa, T. Hashimoto, *Macromolecules* 41 (2008) 8210.

[121] T. Crisenza, H-J Butt, K Koynov, R. Simonutti, *Macromol Rapid Commun*, (2011) DOI: 10.1002/marc.201100622.